universität wien

MASTERARBEIT / MASTER'S THESIS

Titel der Masterarbeit / Title of the Master's Thesis

„Resolving the structure and function of the intestinal microbiota at a fine spatial scale“

verfasst von / submitted by

>Owen Williams BSc<

angestrebter akademischer Grad / in partial fulfilment of the requirements for the degree of

Master of Science (MSc)

Wien, >2016< / Vienna >2016<

Studienkennzahl lt. Studienblatt / degree programme code as it appears on the student record sheet:	A >066 830<
Studienrichtung lt. Studienblatt / degree programme as it appears on the student record sheet:	Molekulare Mikrobiologie, Mikrobielle Ökologie und Immunbiologie
Betreut von / Supervisor:	>Assoc.-Prof Dr Alex Loy<
Mitbetreut von/ Co-Supervisor:	>Assoc.-Prof Dr David Berry<

“For nitrates are not the land, nor phosphates; and the length of fiber in the cotton is not the land. Carbon is not a man, nor salt nor water nor calcium. He is all these, but he is much more, much more;”

John Steinbeck in “The *Grapes of wrath”* 1939

“*It is important to remember that some bacteria are useful”*

Ely Metchnikoff in “*The prolongation of life; Optimistic studies”* 1907

“*Tell me…….”*

Orest Kuzyk, all the time.

Table of Contents

Introduction.....7

Materials and Methods.....14

Immuno-histology staining and spatial organisation of Muc2 Mucin.....14
Methacarn fixation and laser micro-dissection.....14
DNA extraction and PCR.....16
dithiobis(succinimidyl propionate)(DSP) as a fixative for FISH protocols.....17
Fluorescence in situ hybridisation comparison of PFA and DSP fixation on faecal homogenates.....17
Immune-histology staining of Muc2 on DSP fixed colonic sections..... 18
Mapping Akkermansia across a fixed colon section.....18
Semi-quantitative distribution of Akkermansia in colons of mice on two diets.....21
FISH probe design against the **Erysipelotrichaceae** ***family***.....22
In silico FISH probe design.....22
In vitro probe evaluation.....24
Mucinase assay development.....24
Free sugar release assay.....24
N-acetyl neuraminic acid (NANA) release assay.....25
Anthocyanin intervention and human faecal investigation.....25
Participants and collection.....25
Microbial DNA extraction.....26

Results.....27

Immuno-histology staining and spatial organisation of Muc2 Mucin..... 27
Methacarn fixation and laser micro-dissection.....27
DNA extraction and PCR.....28
dithiobis(succinimidyl propionate)(DSP) as a fixative for FISH protocols.....29
Fluorescence in situ hybridisation comparison of PFA and DSP fixation on faecal homogenates.....29
Immune-histology staining of Muc2 on DSP fixed colonic sections.....33
Mapping Akkermansia across a fixed colon section.....34
Semi-quantitative distribution of Akkermansia in colons of mice on two diets.....38

FISH probe design against the **Erysipelotrichaceae** ***family***.....42

In silico FISH probe design.....42
In vitro probe evaluation.....42
Mucinase assay development.....47
Free sugar release assay.....47
N-acetyl neuraminic acid (NANA) release assay.....52
Anthocyanin intervention and human faecal investigation.....52

Discussion.....53

Immuno-histology staining and spatial organisation of Muc2 Mucin.....53
Methacarn fixation and laser micro-dissection.....53
DNA extraction and PCR.....53
dithiobis(succinimidyl propionate)(DSP) as a fixative for FISH protocols.....54
Fluorescence in situ hybridisation comparison of PFA and DSP fixation on faecal homogenates.....54
Immune-histology staining of Muc2 on DSP fixed colonic sections.....55
Mapping Akkermansia across a fixed colon section.....55
Semi-quantitative distribution of Akkermansia in colons of mice on two diets.....57
FISH probe design against the* Erysipelotrichaceae *family.....59
In silico FISH probe design.....59
In vitro probe evaluation.....60
Mucinase assay development.....61
Free sugar release assay.....61
N-acetyl neuraminic acid (NANA) release assay.....63
Anthocyanin intervention and human faecal investigation.....65

Conclusions.....65

Zusammenfassung.....66

Glossary of terms.....67

Bibliography and References.....68

Acknowledgments.....72

Curriculum Vitae.....73

Introduction

Microbial ecology as a separate discipline is fairly new in the scientific community, however it's ancestry can be traced back to the early part of the 20th century and the father of modern microbial ecology Ely Metchnikoff. In his 1907 book „*The prolongation of life: Optimistic studies* "Metchnikoff asses the role of intestinal flora on health and longevity on the host. The conclusion made is that the vast majority of intestinal bacteria are detrimental to human health and shorten life expectancy with the exception of a few choice *Lactobacilli* species. In his book, Metchnikoff focuses on the apparently high proportions of centenarians among peasant populations in rural Bulgaria in which a sour milk product, "*yahourth*" is a staple of the local diet. *Lactobacillus bulgaricus*, as it was named by Grigorov, was found in high numbers in this milk product and due to its high lactic acid production was theorised by Metchnikoff to be a contributing factor to the longevity of the population, by replacing harmful species in the colon with the more "benign" *L. bulgaricus*.

With this publication Metchnikoff began a line of scientific inquiry which continues to this day, by establishing, albeit theoretically, a link between diet, specific bacterial species, intestinal communities and human health. As is often the case in modern science, the more that was elucidated about the human microbiome the more it was realised how complex the system is. Modern use of genome sequencing (of both the host and the microbiome) has established a massive database of host variations and also a huge diversity of uncultured bacteria found in the human gastro-intestinal (GI) tract (**Stevenson *et al.* 2004**). Correlating host diversity, the variety of bacteria found in the intestine (as well as proportions of them to each other) and the notoriously variable human diet with health and pathology in the host is a daunting task. Investigating any of these variables alone requires great computing power and perseverance, finding correlations between them is even more difficult.

In the last decade an intense target for investigation, regarding human health, has been the interaction of gut microbiota, the microbial commensal communities in the colon, with the host. It has become clear that an increasing variety of chemical and physical interactions between humans and gut microbiota take place to ensure a delicately balanced state of intestinal health. The interface between these, evolutionarily diverse, organisms is the intestinal epithelium layer, with alterations in either host features or gut microbiota composition being implicated in a variety of pathologies including;

cardiovascular disease (**Wang *et al.* 2011**), irritable bowel syndrome (IBS; **Ouwerkwerk, de Bos and Belzer 2013**) and even obesity (**Koeth *et al.* 2013, Everard *et al.* 2013**). One species of particular importance to gut health is *Akkermansia muciniphila* found in both humans and mice, making it an important model for investigating human-microbe interactions whose presence or absence is associated with some important pathologies (**Everard *et al.* 2013**). *A. muciniphila* is one of several gut microbes shown to be able to colonise and utilize the relatively harsh niche within the mucus layer found coating the intestinal tract (**Berry *et al.* 2013**), a potentially critical niche for both host and microbial community. The mucus layer contains rapidly fluctuating redox microenvironments and host immune molecules, as well as having a high flow rate.

The human, as well as murine, gastrointestinal tract is, in healthy individuals, coated with a complex mixture of mucin proteins, secreted from goblet cells into the lumen. The entire GI tract is coated with a layer of mucus comprised of various cell surface attached and excreted mucin proteins MUC1, MUC2, MUC3 A, MUC3B, MUC4, MUC5AC, MUC12, MUC13, MUC15, MUC17 and MUC20 localised in various anatomical and topographical areas in the GI tract, with MUC2 being the predominant mucin in the colon (**Linden *et al.* 2008**). The mucus layer itself can range in thickness up to a maximum recorded 800 μm in the rodent rectum (**Atuma *et al.* 2001**) and is composed of two distinct layers, the inner and the outer mucus layer (**Ouwerkwerk, de Bos and Belzer 2013**). Bacteria able to colonise this layer are of great interest as they may be regulators of human-flora interactions due to the fact that mucin degrading bacteria may be less transient residents in the gut owing to their feeding on a source of energy and nutrients whose availability is independent of the host diet, i.e. mucus.

The role of the intestinal mucus layer is wide reaching but mainly is thought to act as a physical barrier between the intestinal epithelia and the bacteria in the lumen. Mucins are either secretory molecules which interact with each other forming a thick gel structure (Figure 1), they may also be membrane bound such as MUC4 and MUC16 and thus form the densely packed glycocalyx (**Davies, Wickström and Thornton 2012**).The primaryfunction as a barrier is partly achieved by mucin's size and structure, being large branched glycoproteins with high numbers of *O*-linked glycans chains combining to form a glycosylated molecule of up to 2.5 MDa which interacts to form vast networks (**Johansson *et al.* 2008**). This dense gel on the epithelia also physically prevents penetration by pathogens through its continuous flow through the colon. Mantel and Husar (**1993**) showed that adding virulence factor containing- plasmids to epithelia-penetrating pathogens reduced bacterial binding to the mucus, and theorised that this allows pathogens to overcome clearing by the flow of mucus.

The sheer size of mucin molecules, and their tendency to cross link with each other makes the mucus-gel layer a formidable barrier to microbial penetration. The closer the proximity to the epithelial layer the denser the mucus becomes, and is thus shown to contain two distinct layers. The inner most layer, immediately covering the epithelia is tightly packed and more difficult to remove than the outer layer,

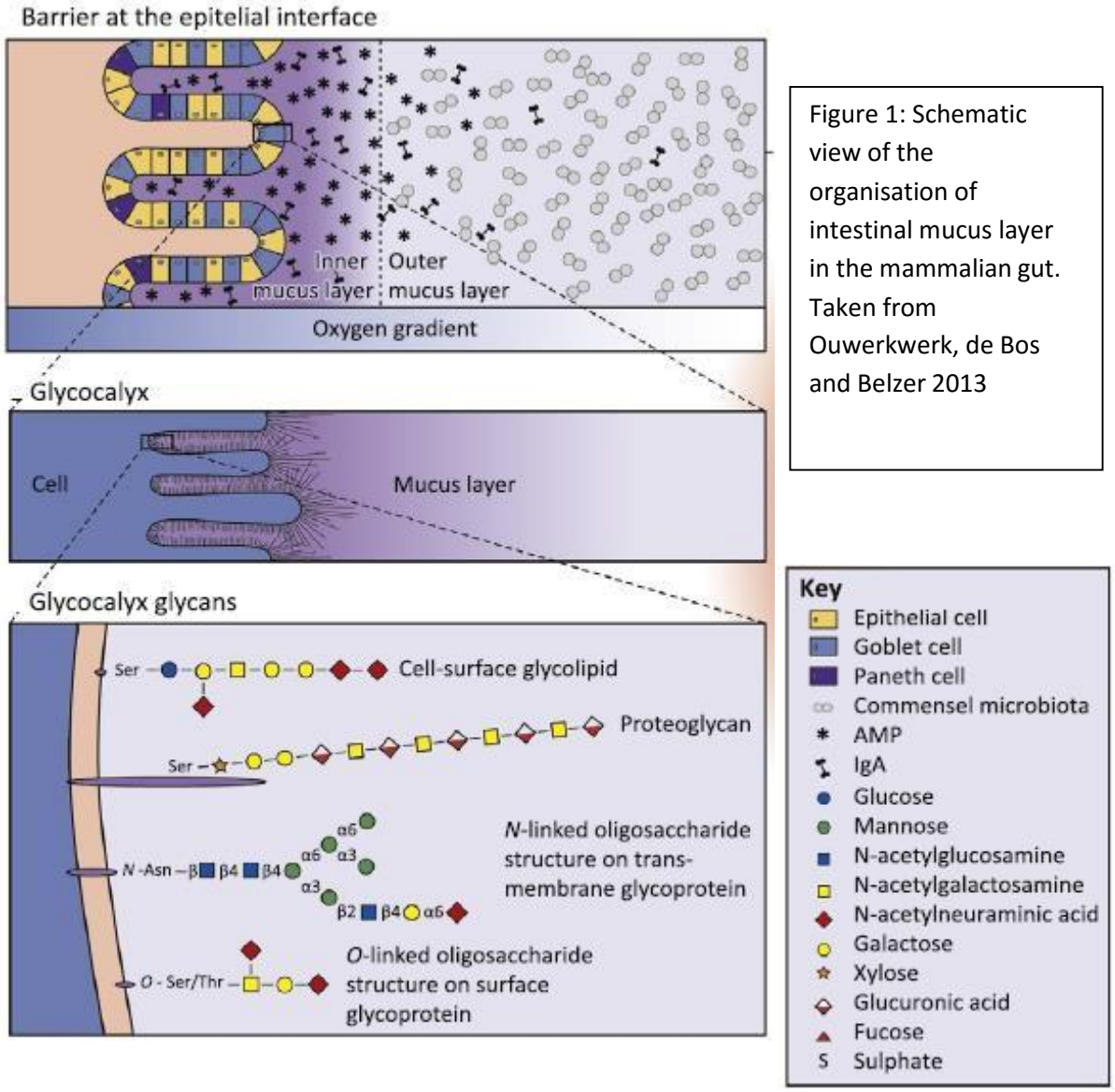

Figure 1: Schematic view of the organisation of intestinal mucus layer in the mammalian gut. Taken from Ouwerkwerk, de Bos and Belzer 2013

based on this the two layers are known as the inner and outer mucus layers. The transition from the densely packed inner layer to the looser outer layer was shown to be mediated by proteolytic cleavage of mucins as it is secreted into the lumen (**Johanssen *et al.* 2008**). The origin of these proteases is debated, and could come from microbial partners in the gut or, alternatively, from the host. The inner mucus layer has often been shown to be sterile (**Johanssen *et al.* 2008**) whereas the outer is colonised by commensals. One factor contributing to the sterility of the inner mucus layer is a steady increase in oxygen concentrations towards the epithelial layer. As most intestinal bacteria species are strict anaerobes and are therefore unable to establish colonies (**Kahn *et al.* 2012**).

On top of all these hostile factors in the mucus layer, secreted immune- globulins (IgA) are found in high numbers in the outer mucus layer, which seems to select which bacteria are admitted into the mucus, thus selecting for commensals and against pathogens (**Rogier *et al.* 2014**).

The mucosal interface between host and bacteria is also of vital importance to development and maintenance of a normal immune response by the host (**Garcia-Garcia, Galindo-Villegas and Mulero 2013**). Initial colonisation of the gut after birth is a critical time for the immune system by resisting pathogen infection but also in "priming" the immune system (**Galindo-Villegas *et al.* 2012**). Theoretically we could consider bacterial species residing so close the host immune apparatus, i.e. in the mucus, as acting as indirect markers for commensal communities in the rest of the gut. In this case the production and maintenance of a mucus layer acts to keep the majority of species "at arm's length" to prevent an over-activation of the immune system by the general bacterial milieu. Loss or reduction of the mucus layer causes the immune system to be activated inappropriately by bacterial agents in the lumen causing chronic inflammation of the epithelia, implicated in IBS (**Ouwerkwerk, de Bos and Belzer 2013**), colo-rectal cancers (**Belcheva *et al.* 2014**) and even psychological pathologies such as depression (**Janos, Illes and Balacco-Corrado 2011**). The mucus layer is also important in protecting the epithelium layer from the harsh digestive enzymes released into the colon itself (**Qin *et al.* 2011**). An inflamed gut barrier is implicated in increased permeability of the barrier layer, allowing easier entry routes for pathogens, potentially harmful molecules and also increased calorie intake across the gut leading to obesity.

The presence of fermentative bacteria in the lumen gives rise to a wide variety of by-products that may be beneficial to the host. Some of these by- products may be active molecules that directly affect the host such as ellagitannins which are produced from dietary sources and actively scavenge free-radicals thus mitigating their effect on the host (**Fridrich *et al.* 2008**). Other products can also interact directly with cells through receptors such as glucosinolate break-down products which actively inhibit colon, breast and prostate cancers (**Traka *et al.* 2008**). More commonly however, bacterial fermentation products also act as energy sources for the intestinal epithelia. Fermentation of dietary fibres results in the release of short-chain fatty acids (SCFAs) such as Butyrate, propionate and acetate, which in turn are the primary energy source of intestinal epithelia cells (**Ottman *et al.* 2012**). The absence therefore of bacteria, such as in gnotobiotes or animals undergoing antibiotic treatment, can have wide-ranging effects on intestinal tissue health. To that effect the presence of certain species in close proximity to the epithelia has been shown to increase the thickness of the mucus layer and subsequently may be implicated in improved intestinal and general health. Everard *et al.* (2013) showed that supplementing mouse diet with viable

Akkermansia muciniphila populations increased the thickness of the mucus layer which in turn correlated with lower levels of obesity in mice fed on a high fat diet.

A. muciniphila is a gram negative anaerobe in the *Verrucamicrobia* phylum which is found in both human and mice, making it a good research candidate for medical investigation into several intestinal or intestinal associated pathologies. In addition to Everard *et al.*'s 2013 paper establishing a negative correlation between *A. muciniphila* numbers and obesity in mice, *A. muciniphila* has also been shown to reduce intestinal inflammation (**Karlsson *et al.* 2012**) which has implications not only on weight gain, but also Irritable bowel disease, cancers and multiple organ dysfunction syndrome (MODS) as the intestines become more permeable to chemicals and enzymes from the GI tract (**Qin *et al.* 2011**). As *A. muciniphila* is able to utilise mucins as its sole carbon source and is abundant (up to 3% of total bacterial load) it has an implied significance in the healthy human GI tract (**van Passel *et al.* 2011**).

Isolating mucus associated bacteria *in situ* from the mucosal layer allows us to study their distribution in regard to the host and also other microbial players, and to observe the effect, if any, diet has on their composition within the gut community. We would like to attempt the immunohistological staining of mucins in conjugation with fluorescence *in situ* hybridisation (FISH) on fixed cecal or colonic sections to allow visualisation of *A. muciniphila* in regards to the proximity to the intestinal epithelium. FISH probes are used to target the 16S ribosomal RNA sequences, which allow distinction of bacterial species. Laser-assisted micro dissection (LMD) also allows the isolation of these bacteria for genomic analysis. However traditional fixation methods, such as paraformaldehyde (PFA) fixation, make mucus immunohistological analysis difficult due to loss of the highly hydrated mucus layer during PFA fixation and also affects downstream nucleic acid recovery due to extensive cross-linking between biomolecules (**Xiang *et al.* 2004**). To overcome these obstacles Xiang *et al.* propose using dithiobis (succinimidyl propionate) (DSP) as an alternative fixative (Figure 2). DSP was shown to be able to fix tissues by binding to primary amine groups and not chemically modifying nucleic acids.

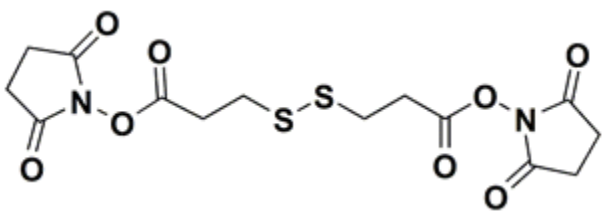

Figure 2. Structure of dithiobis (succinimidyl propionate), or DSP, used in this study as a fixative. After fixation the molecule can be cleaved through the sulphide bridge by addition of dithiothreitol (DTT).

Furthermore, DSP is a reversible fixative and the disulphide bond in the linker chain can be cleaved by the addition of dithiothreitol (DTT) allowing for extraction of freed nucleic acids that can be subsequently amplified via the polymerase chain reaction (PCR). The potential advantage of using this fixative is that it will allow us to reversibly-fix colonic tissue and perform bacterial-FISH staining. Using the FISH staining results as a guide we can micro-dissect areas of interest and sequence 16S rRNA genes allowing for a micro-scale map of which species are found where and in what number.

The principle behind Fluorescence *in situ* hybridisation (FISH) has been known for some time. The technique was developed in the 1969 paper by Gall and Pardue in which radio-labelled RNA molecules were complementarily hybridised with fixed DNA and visualised via autoradiographs, the principle remains essentially the same. In this study DNA FISH probes were designed to be complementary to 16s sub-unit ribosomal RNA (16S rRNA) of a particular bacterial species, genus or family. The RNA probes are joined to a fluorophore which allows for visualisation of the probe position using fluorescence microscopy. Designing a probe that is specific for a bacterial genus or species is a process requiring high computational power. Typically, a FISH probe is 18-20 nucleotides long and must be perfectly complimentary to a sequence in the target groups 16S rRNA structure, but not to sequences in other non-target organisms. As well as the sequence of the probe itself, fidelity can be improved for the target using differing formamide (FA) percentages in the hybridisation buffer. Higher FA% increase the likelihood of the rRNA/FISH probe complex melting, therefore the FA% must be investigated to determine the optimal FA% where the target complex remains hybridised, however organisms with similar rRNA sequences will have a lower melting FA% and therefore will not remain hybridised. Stringency of a FISH probe can be calculated and improved *in silico* but must also be proved *in vitro* before a probe can be deemed useful. In this thesis we developed a FISH probe for a group of organisms of which currently no probe is available. The family *Erysipelotrichaceae,* within the *Firmicutes,* is a group that we have seen in increased numbers of sequence reads from material within the colons of mice fed on either a polysaccharide-free diet or a high fat containing diet. Using the “Arb” database (arb-silva.de) we also here attempted to design a probe using partial sequences from previously sequenced data.

As stated above, the human gut microbiome is potentially of great clinical significance and is itself heavily dependent on diet. By associating specific consumed food-stuffs with clinical parameters and bacterial population changes we may be able to produce pharmaceutical or dietary interventions of significant benefit to human health. In this study we also begin to attempt to investigate the effect of anthocyanin on the gut microbiota and correlate this with specific immune responses in the human host.

Specifically, anthocyanin has been shown in increase expression and activation of the *nrf2* gene in the human host which is involved in the oxidative stress response of host cells (**Kropat *et al.* 2013**). The aldehyde, phloroglucinol (PGA) is produced by intestinal microbiota as a breakdown product of anthocyanin is thought to be the activator of *nrf2* after absorption by the host. To investigate this we sequenced the 16S rRNA genes from human faecal donors who had dietary interventions with anthocyanin enriched fruit juice and donated faeces on day 0 and day 56 of this intervention in an attempt to implicate the microbial players performing this potentially beneficial function.

The final string of this thesis was in beginning to establish a working protocol for a Mucinase assay, which could be used on faecal matter or colonic material to determine which species are able to utilise mucin as a substrate. As mucus is a mixture of complex structures, some up to 10^6 kDa (**Dwarakanath *et al.*. 1995**), there are many possible methods by which intestinal bacteria may be able to use it as a substrate by cleaving molecules or branches of the structure. A range of enzymatic pathways are therefore candidates for mucin degradation, alone or in combination with others. Based on the structure of mucins we can assume possible roles for sulphatases, O-acetyl esterases, sialidases and glycosidases (**Dwarakanath *et al.* 1995**), or a combination. We focused on attempting to detect the breakdown of mucins using two assays. The first was a broad-range assay to determine the release of free sugar molecules from mucin/ faecal incubations and spectrophotometric detection with 3,5-Dinitrosalicylic acid (DNS) at 540 nm. The second assay uses an assay established by Kim and Cha (2002) for detecting the breakdown product, N-acetyl neuraminic acid (NANA), formed after mucin degrading *Vibrio* species cleave the side-chain peptide from the oligosaccharide chain in mucins. NANA can be directly detected spectrophotometrically at 280 nm. The aim was to develop a Mucinase assay that could be used on microtiter plates without the need for complex radio-labelled- threonine mucin substrates such as those used in Dwarakanath *et al.* 1995.

Therefore the aims of this thesis were to examine the effectiveness of the novel fixative DSP in regards to FISH preparation and subsequent PCR of micro- dissected colon samples from mice, and then to use this new fixative to assess community composition and locational information of *A. muciniphila*. To design a novel and functional FISH probe for the *Erysipelotrichaceae* family group of bacteria associated with our diet experiments, and finally to investigate assays which may be used to quickly detect Mucinase activity of cultures or faecal matter.

Materials and Methods

Immuno-histology staining and spatial organisation of Muc2 Mucin

Methacarn fixation and laser micro-dissection

As a preliminary study we made, using an histology microtome (Leica), 5 µm thick histology sections of methacarn fixed (a modified form of Carnoy's fixative using methanol instead of ethanol) mice intestines. These were to be stained with FISH probes and immune-histology staining of the Muc2 mucus protein since alcohol fixation is the preferred method of hydrated mucin preservation (**Johansson & Hansson, 2011**). Sections were mounted onto UV- treated polyethylene terephthalate (PET) 1.4 µm thick LMD slides (Leica) before undergoing a de-waxing process: Slides were incubated at 60^{o}C in xylene for 10 min and then at room temperature in xylene and a final immersion in dry ethanol, room temperature, for 5 min.

Muc2 was immune-histo-stained using rabbit anti-Muc2 H300 antibody (Santa Cruz 1:200 in blocking solution-1%BSA in PBS) overnight at 4^{o}C and then incubated for 1 hour with 1:1000 (in blocking solution) anti-rabbit Cy3 labelled antibody at 4^{o}C. After this, sections were stained with a 1:1000 DNA stain, 4', 6 diamidino-2-phenylindole (DAPI) solution, (in PBS) for 15 min at room temperature in the dark, and washed in chilled MilliQ water. We then micro- dissected mucus stained samples with the aim to PCR amplify the 16S rRNA gene of any bacteria within this layer. On the visualised sections, using the Muc2 stain as a guide, four 10,000 µm^2 sections were dissected of areas containing only mucus close to the epithelial layer, two 10,000 µm^2 sections containing both the mucus layer and luminal content, extending no more than 100 µm into the lumen. Additionally, two 10,000 µm^2 sections were dissected of just luminal contents and two 10,000 µm^2 sections from outside the sample as a negative control, all shown in Figure 3.

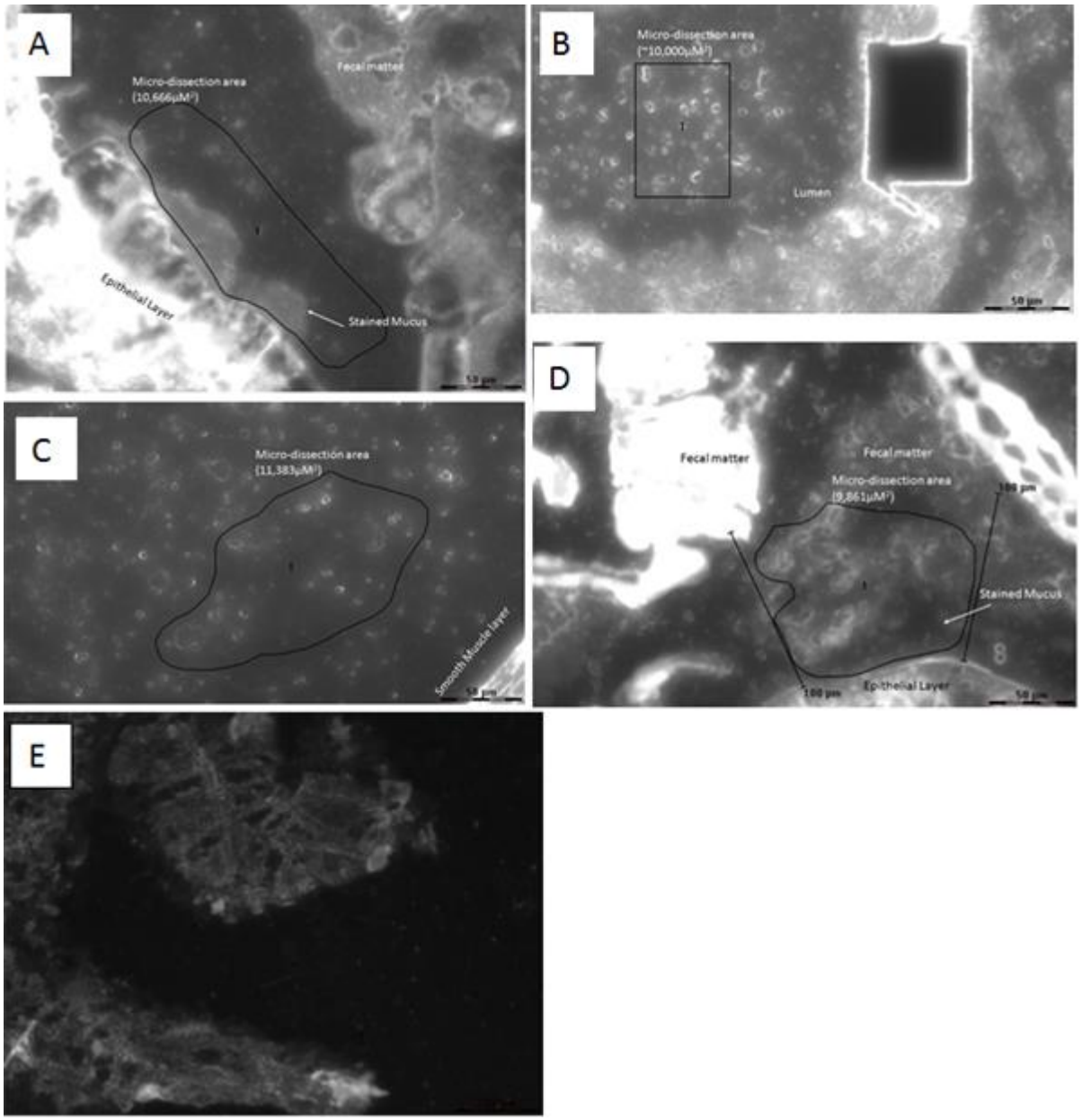

Figure 3. LMD images of micro-sections before cutting showing Muc2 stain areas visualised in the DAPI channel. The high background in these images is partly due to auto-fluorescence in the sample. Muc2 staining, in the Cy 3 channel, guided target acquisition, and these images are taken in the DAPI channel. A: sections from the mucus layer. B: Empty membrane from outside the section. C: Luminal content section. D: Section proximal to the epithelium layer encompassing the mucus layer and the luminal contents. E: Negative control section stained with the secondary Muc2 antibody but not the first, image taken in the Cy3 channel

DNA extraction and PCR

Sections were captured in UV treated, tissue lysis buffer (ATL) (from the Qi Amp mini DNA extraction kit, Qiagen) and DNA was extracted using the Qi Amp mini DNA extraction kit according to the manufacturer's instructions. V3- V5 variable regions of bacterial 16S rRNA gene sequence were amplified in a 2 step PCR reaction with headed, 341F and 785R primers and barcoding primers (Figure 4). Each sample contained 5 µl of extracted DNA product, along with 15 µl of the following master-mix; 2 µl 10X Taq buffer, 2 µl 2 mM deoxynucleotide mix (dNTP), 1.6 µl 25 mM $MgCl_2$, 0.4 µl 50 µM primer solutions of both forward and reverse headed primer, 0.1 µl 20µg/ml bovine serum albumen (BSA), 0.1 µl 5 U/µl Taq polymerase and 8.4 µl PCR-grade water. The samples underwent a 10 repeat PCR cycle as follows; 95°C incubation for 3 min, 95°C for 30 s, 55°C for 30 s, 72°C for 1 min, with a final 72°C phase for 7 min. Of the resulting product 2 µl were transferred into 18 µl of the above master-mix and run on a 30 repeat cycle PCR programme as above, excepting a 52°C instead of 55°C 30 s step.

The PCR product was analysed by running it on a 1.5% agarose gel (Figure 4).

HBact341F	GCTATGCGCGAGCTGCCCTACGGGNGGCWGCA
HBact785R	GCTATGCGCGAGCTGCGACTACHVGGGTATCTA
barcoding primers:	xxxxxxxxGATGACCTGCTATGCGCGAGCTGC
Bact341F	CCTACGGGNGGCWGCAG
Bact785R	GACTACHVGGGTATCTAATCC

Figure 4. Primer sequences used in all PCRs. Red indicates adaptor sequences, green reverse adaptor sequences and x's denote unique 8-nt long barcode sequence.

Furthermore, as part of this investigation a high amount of contamination was observed in subsequent PCR reactions and we set about using guide-lines in Champlot *et al.* 2010 to reduce them (see below). To asses this, LMD micro-sections were created of blank LMD slides and before 16S rRNA PCR runs, a small volume of 5 µg/µl faecal homogenate was added to samples. DNases were added to BSA before PCR reactions were started and non-nucleic acid PCR reagents were subjected to 15 min UV cross-

linker treatment. PCR products were then run on 1% agarose gel to determine the success of contamination reduction (Figure 9).

dithiobis(succinimidyl propionate)(DSP) as a fixative for FISH protocols

Fluorescence in situ hybridisation comparison of PFA and DSP fixation on faecal homogenates

To evaluate the performance of DSP as a fixative for use in FISH analysis, we compared the results of a DSP fixation step and that of the standard fixative for such procedures, PFA. To achieve this, faecal pellets from lab-bred mice were homogenised at 4˚C in phosphate buffered saline (PBS solution) before being centrifuged at 4˚C at 700 X *g* for 30 s, after which the pellet was discarded. The supernatant was split into equal fractions to be fixed in either DSP or PFA and centrifuged again at 4˚C and 4000 X *g* for 10 min. The resulting pellets were re-suspended in 200 µL of either 2 mM DSP/PBS solution for 20 min, followed by a 10 minute Tris wash, or 4% PFA/PBS solutions for 30 min. Fixed samples were then centrifuged again for 10 min at 4˚C and 4000 X *g* and the pellets re-suspended in 500 µL PBS solution, and centrifuged as previously. The resulting supernatant was spotted onto glass FISH slides.

The fixed samples were then subject to a variety of FISH probe hybridisations. Slides were washed for 3 minutes in 50% ethanol and subsequently for the same time period in 80% and finally 96% ethanol to remove water. After this, hybridisation buffers compatible with the FISH probes to be used were produced with corresponding formamide (FA) percentages (see below). The FISH probes used target specifically the 16S rRNA sequences of the named species or groups. Two µL of 5 µM FISH probe were added for each section and the hybridisation buffer was added to bring the final volume to 20 µL. The slides were placed in a 50 mL Falcon tube with tissue paper soaked with ~900 µL of hybridisation buffer and incubated at 46˚C for 2 hours.

To compare FISH staining efficiency (coverage and intensity) of faecal homogenate fixed with either DSP or PFA, the following probes were used: *Akkermansia* 1437 Cy3 DOPE probe, with EUB338 I-III, Fluos DOPE probes at 30% FA. This section was used to evaluate an *Akkermansia* stain against total *Bacteria* stain, of which *Akkermansia* should also be stained. A second series of samples was stained as follows; with EuB338 I-III Fluos DOPE combined with Baci 731AB Cy5 DOPE at 35% FA. Baci 731AB probe targets *Bacteriodes acidifaciens*, a common Gram-negative gut microbe. All samples were also stained with 4', 6 diamidino-2-phenylindole (DAPI) DNA stain for 15 minutes.

The hybridization images (20 images) were acquired using a confocal laser-scanning microscope (CLSM-Leica) and images of the samples were analysed using the DAIME programme to evaluate coverage. The results are shown in Figure 10. DAIME percentages coverages were conducted using the "edge detection" feature which determines the cut-off for an object in an image to be counted as a signal. In the first of such experiments the edge detection was set to 30 and then repeated at 70 to evaluate whether altering the cut-off stringency effects the results, these are shown in Figure 11.

Immune-histology staining of Muc2 on DSP fixed colonic sections

To evaluate whether DSP fixation has an impact on immune-histology staining we used antibodies directed against Muc2 on 16 µm thick sections of proximal and distal colon from mice on normal chow diets. Colon sections were removed after the mice were sacrificed and immediately embedded in optimal cutting temperature (OCT) medium (Neg 50- Richard Allen scientific) and stored at -80^{o}C until needed. Sections were made using a cryotome at -24^{o}C and mounted on UV treated glass microscope slides. Sections were fixed using a 2 mM DSP-DMSO solution for two incubations at room temperature for 30 min each, followed by a brief PBS wash, and finished with a 15 min incubation in 1 M sterile TRIS solution. Slides were then dehydrated using 3min room temperature incubation in 50% ethanol, followed by 80% and 96% ethanol solutions and left to dry.

FISH staining was performed as above using the probe Akk1437 Cy3-DOPE and a 30% FA hybridisation buffer. After FISH staining the sections were stained with the general DNA stain, Sybr green (Qiagen) in a 1:10,000 dilution in MilliQ water for 15 min in the dark. After this, the sections were immune-histologically stained as above with secondary antibodies also containing a Cy3 fluorophore. The results of these incubations are shown in Figure 13

Mapping Akkermansia across a fixed colon section

The proximal colon of a C57BL/6 mouse, fed on powdered normal mouse chow (ssniff) was excised after sacrificing and immediately frozen in OCT until needed. This colon (approx. 4 cm long) was cleaved in two using a microtome blade while still frozen in OCT (see Figure 5). In contrast to previous methods here, these two colonic "halves" were fixed whole in either DSP of PFA.

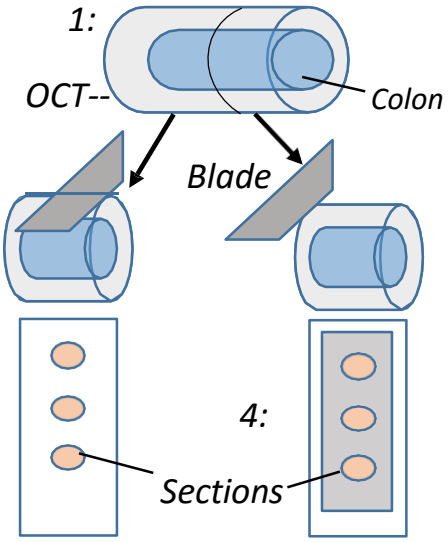

Figure 5. Experimental set-up using powder-fed mouse colon. 1: Whole colon is frozen in OCT on excision from sacrificed mouse, and then cleaved in two using microtome blades. 2: one half is fixed in PFA (see text) and one in DSP, and re-frozen in OCT and from both, sections are made using a cryotome.
Sections are taken a few µm away from the site of the original bisection so as to ensure the two sets of sections will be ~50 µm downstream of each other. 3: PFA sections are placed on glass CLSM slides. 4: DSP sections are placed on PET LMD

The two colon halves were fixed in either 4% PFA/PBS or 2 mM DSP/PBS for 6 hours at 4°C and then transferred to a 20% sucrose solution over night at 4°C to prevent crystallisation. Ten µm thick sections of each treatment were made using a cryotome apparatus and sections stored on either glass slides (PFA fixed) or LMD slides (DSP). The PFA fixed sections were FISH stained and used to map *Akkermansia* populations across the entire section. One DSP fixed section slide was stored at -20°C for further analysis (see "*semi-quantitative distribution of Akkermansia in colons of mice on two diets"*).

The PFA fixed sample was hybridised for FISH probes (using the protocol above) using the EuB338 I -III Fluos DOPE and Akk435 Cy 3 DOPE probes and DAPI DNA stain. An entire section was visualised using a CLSM (Leica) and images evaluated using the DAIME software to evaluate *Akkermansia* populations (Figure 14). Images were sorted into either "epithelia", where any amount of epithelial structure was visible, or "luminal", where no epithelia were visible.

One section of DSP fixed material on an LMD slide remained unstained and 10,000 μm^2 micro-sections were dissected from the entire section (Figure 6) and captured in UV treated ATL buffer as before.

A) B)

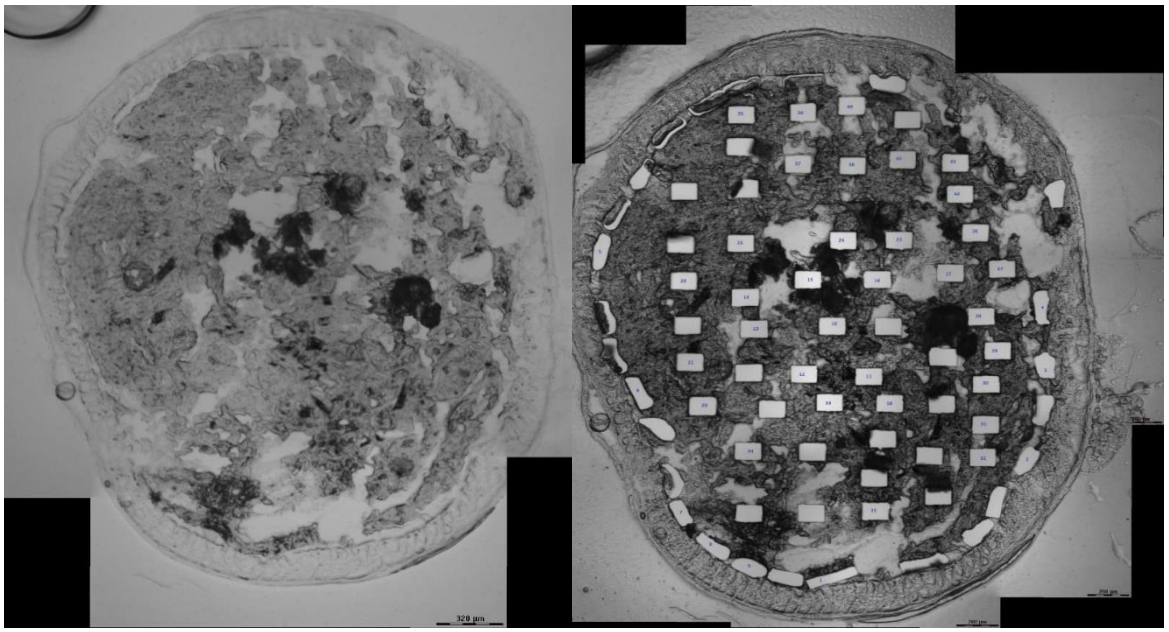

Figure 6. Composite image of DSP fixed colon section before micro-sectioning (A) and after (B). Each section was captured in a separate PCR tube containing 26 µl of ATL buffer and stored at -20^{o}C until needed. Micro-sections are given a numerical designator allowing PCR results to be related back to the micro-geography of the section. 9 micro-sections were taken from the epithelial-proximal area and a further 33 micro-sections taken at random from the lumen. Not all micro-section captures were successful and were abandoned.

Samples captured in ATL buffer were extracted as before and subject to PCR amplification in the same master mix environment and cycle set up as previously. These samples were subject to a 20 cycle initial PCR set-up using general 16S primers; HBact 341F and HBact 785R and 2 µl of the subsequent product underwent a further PCR set-up of 10 cycles using individually allocated barcode primers. All samples were subjected to a magnetic bead- PCR clean up set using the Agencourt magnetic bead clean-up protocol. Sample concentrations were calculated using a Pico green assay, after which samples were pooled and sent for sequencing (MiSeq). Populations of *Akkermansia* species reads were calculated as a percentage of total bacterial reads, see Figure 16. The DSP fixed micro-sections also had the *Akkermansia* reads percentages compared to the percentages obtained using the DAIME programme from images of PFA fixed CLSM FISH micrographs (Figure 17).

Semi-quantitative distribution of Akkermansia in colons of mice on two diets

Using sections obtained from the same colon sample as in "*Mapping Akkermansia across a fixed colon section"* fixed in DSP and on the powdered normal chow diet, we also attempted to evaluate the ability of DSP to give semi- quantitative sequence data reads. A second mouse, fed on the pelleted form of normal chow, was sacrificed and its proximal colon also excised and fixed with DSP as before and sectioned onto LMD slides. Powder-fed mice were hypothesised to have a much higher *Akkermansia* population than those mice fed on the pellet form of diet, the aim was therefore to see if sequence data from both DSP fixed colons would reflect the populations seen using FISH stains. Both pellet and powder fed sections were FISH stained as before using only the Akk435 Cy3 DOPE probe and then stained with DAPI. Eleven samples were micro- dissected from each treatment and captured in ATL buffer. Samples were chosen based on amount of Akk Cy3 signal, while confirming that each 10,000 μm^2 micro-section had equivalent DAPI stain coverage (Figure 7).

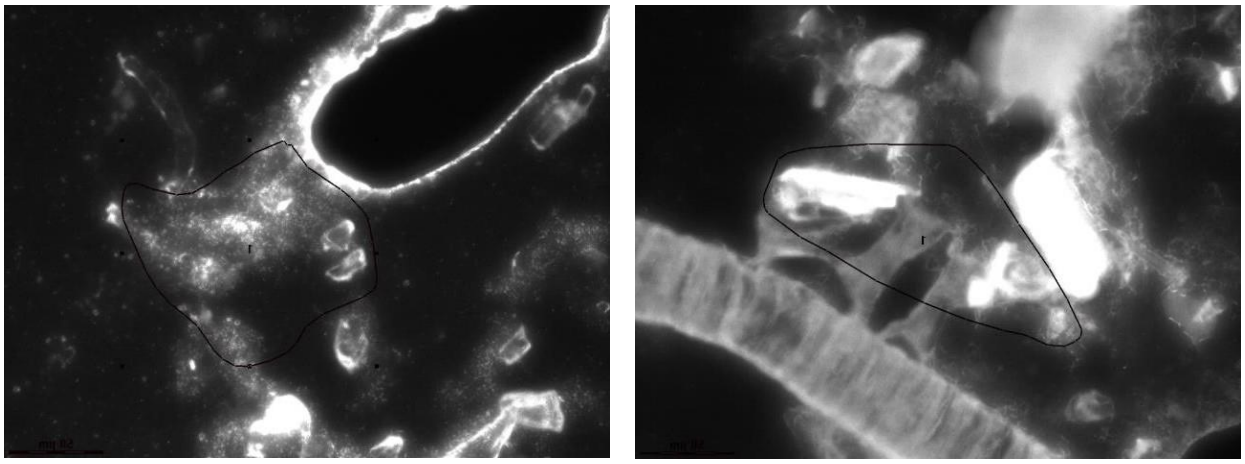

Figure 7. LMD images of sections chosen for micro-dissection. Both mages are in the Cy3 (Akk 435 Cy3 DOPE) channel. Highlighted areas denote the ~10,000 μm^2 micro-sections prior to laser dissection. Left panel is from the powder fed mouse and the right panel is from the pellet fed mouse.

Samples were captured, extracted and subjected to the same PCR protocol as above, including PCR magnetic bead clean-up, and sent for sequencing.

FISH probe design against the* Erysipelotrichaceae *family

In silico FISH probe design

Oligonucleotide FISH probes were designed against the genus *Allobaculum* based on the non-redundant ARB-SILVA database version 119.1 (http://www.arb-silva.de/) using the probe tools of ARB (**Ludwig et al. 2004**) and probeCheck (**Loy et al. 2008**). The *in silico* probe candidates are summarized in Table 1.

Table 1. 16S rRNA-targeted oligonucleotide probes for fluorescence in situ hybridization.

Probe name	Full probe name[1]	Probe sequence (5'-3')	FA [%] (Perfectly-matching type strain used for testing)	Perfectly matched target organisms/sequences	ΔG: Free energy for perfect match hybrid [kcal/mol][2]	RDP II probe match[3]	
						Coverage	Number of non- target hits
ALBA365	S-F-ALBA-0365- a-A-18	TTG CGC CCA TTG ACG AAA	Unknown	*Allobaculum* family	-20.03	*Allobaculum* 770 Target Hits (92%)	322
c1ALBA365	-	TTG CGC CCA TTG ACG AAG	Unknown	Competitor for ALBA365	-20.03		

[1] According to Alm et al. 1996.

[2] Calculated using the default settings in probeCheck (http://www.microbial- ecology.net/probecheck).

[3] RDP II probe match was performed with database release 11, Update 4 (May 26, 2015) containing 3,224,600 bacterial and archaeal 16S rRNA sequences. The search for each probe was restricted to sequences of good quality with data in the respective probe-binding region. Coverage is the percentage of sequences within the RDP II target taxon that shows a full match to the probe sequence. The number of non-target hits indicates the total number of sequences outside the respective RDP II target taxon that shows a full match to the probe sequence.

The optimal formamide concentration to use is one aspect we hope to determine in the course of this study.

In vitro probe evaluation

The FISH probe ALBA365 was chosen to be investigated as it had the most suitable coverage of the *Allobaculum* genus a member of the *Erysipelotrichaceae* family. ALBA365 was also evaluated using "Mathfish" online resource which calculates theoretical Formamide percentages to be used in FISH hybridisations. Mathfish calculated a probe with optimal FA% of 15% which would allow a stringent hybridization excluding non-target mismatches from being labelled. It was decided to test the probe using 0%, 10%, 20%, 30%, 40%and 50% FA% to determine optimal concentrations. For this evaluation a cecal homogenate (in 50% ethanol/PBS) fixed in PFA from a mouse shown to have high *Allobaculum* representatives from sequence results ("female C" from Buck Hanson's glucose ureide study). ALBA365 in Cy3 and its competitor, cALBA365 – unlabelled, were ordered (Biomers, Germany) and hybridized as described previously with the various sections in conjunction with the EuB338 I, II&III pan-bacterial stain as well as an identical hybridisation without the EuB338 I-III pan-bacterial probes. The reason for this is that it was unknown whether EuB338 I-III would aid or hinder binding of ALBA 365 due to the two probes binding points being so close to each other on the variable region of 16S rRNA (position 338 and 365). Slides were stained with DAPI DNA stain (1:1000 dilution in MilliQ water) and images taken using a CLSM microscope (Leica), and images evaluated using the DAIME FA% function which evaluates signal intensity to determine the optimal FA% for a given probe as well as populations stained by each probe. The results of these hybridisations are shown in Figure 22 and 23.

Mucinase assay development

Free sugar release assay

The substrate used in this assay was Porcine stomach mucus (Sigma) made to 5% w/v in 1X phosphate buffered saline (PBS) and was kept at 4^{o}C until used. One faecal pellet was obtained from mice fed on the same control diet. This pellet was homogenised to 1 mg/50 µl in PBS and split into three aliquots, one of which was autoclaved (autoclaved sample), centrifuged at 400 X *g* for 30 s and supernatant was kept on ice. One of the supernatants was then filtered through a 0.2 µl filter to remove bacterial cells (the filtered sample), leaving an autoclaved, a filtered, and a "pure" sample containing re-suspended faecal matter only. A maltose sugar solution was used as a standard with concentrations at 1000 µg/100 µl, 250 µg/100 µl, 100 µg/100 µl, 50 µg/100 µl, 25 µg/100 µl and 0 µg/100 µl. Porcine stomach mucus (PSM) was diluted to 5%, 2%, 1% and 0% (i.e. only PBS) and 50 µl added to corresponding

wells in a 96 microtiter plate. Fifty µl of each of the three faecal fractions (autoclaved, filtered and pure) were added to 50 µl of each of the mucus dilutions independently, and a final mucus dilution series had 50 µl of PBS added as a control. Plates were incubated with their standard dilutions for either 1 hour or 6 hours at 30^{o}C with shaking at 300 RPM. After incubation of each time point, 100 µl of 3,5- dinitrosalicylic acid (DNS) was added to all samples, transferred to a new plate and incubated for a further 30 min as above. After this time, the plates were incubated in a 95^{o}C water bath for 5 min. One hundred µl of this sample/DNS mix was transferred to another plate and the absorbance of each well was measured in a plate reader at 540 nm. A standard concentration curve was produced and concentrations in each well of free sugar molecules was calculated using this. Based on the results shown in Figure 25, this assay was also repeated with time points at 30 min and 90 min using 5% mucus/PBS solutions (Figure 24).

N-acetyl neuraminic acid (NANA) release assay

An alternative assay was also prepared to detect the release of N-acetyl neuraminic (NANA), if any, with incubation of mucus and faecal homogenates. Faecal pellets were collected and homogenised as above. Porcine stomach mucus (Sigma scientific) was diluted to 1% w/v in 0.02 M Tris-HCl (pH 5.5) solution as per Kim and Cha (2002) protocol. In a 96 well microtiter plate 50 µl of faecal homogenate solutions (or PBS control) were added in triplicate to 50 µl 1% mucus solutions. Plates were incubated at 30^{o}C for either 30 min or 1 hour. Reactions were stopped with the addition 150 µl of 10% w/v trichloroacetic acid and incubated at 45^{o}C for 15 min, after which plates were centrifuged at 1200 X *g* for 10 min. Supernatants were extracted from the plates and transferred to new wells and the absorbance at 280 nm was measured on a plate reader, absorbance values are shown in Figure 26.

Anthocyanin intervention and human faecal investigation.

Participants and collection

For this study, 60 male participants were chosen in the age range 19-50, exclusion parameters were as follows; a body mass index (BMI) over 25, tobacco consumption, use of medications, practice of competitive sports, suffering from metabolic disorders or diseases, deviation from the nutritional requirements, participation in other studies and blood donations.

Participants diets were supplemented with an anthocyanin enriched juice drink or a placebo juice (both produced by Eckes-Granini for the purposes of this study) and stool samples were collected before the beginning of the intervention and after 56 days on the supplemented diet.

Faecal samples were collected by the subjects either in the morning or previous evening prior to delivery in cool boxes to the laboratory. Samples were then aliquoted into 3 ~0.5 ml samples and snap-frozen in liquid nitrogen to be stored at -80^{o}C until analysed.

Microbial DNA extraction

Aliquots of subjects faecal material was stored at -80^{o}C until needed and DNA was extracted using a phenol-chloroform protocol as follows.

Approximately 500 µl of faecal material was transferred into a bead- beater apparatus tube (Mobio, U.S.A) to which 500 µl of phenol-chloroform isoamyl alcohol (25:24:1- pH 8) and 500 µl of cetyltrimethyl ammonium bromide (CTAB) extraction buffer (1:1 CTAB and 240 mM potassium phosphate solution treated with diethylpyrocarbonate (DEPC)) solution was added and pH adjusted to 8. Samples were subjected to bead beating at 5.5 m/s for 30 s and then centrifuged at 13,000 RPM for 5 min at 4^{o}C. After this the upper aqueous phase was transferred to a new sample tube. This was repeated a second time for the remaining material in the bead beater, and the second aqueous phase added to the one previously collected. To the collected phases 1 mL of chloroform isoamyl alcohol (24:1) was added and the samples centrifuged as previously. The upper liquid layer was pipetted off and transferred to a new sample tube and the process repeated with retention of the final upper liquid layer. To this, 0.1 volume of 3 M Na-acetate and 0.6 volume of ice cold isopropanol was added and tubes left at room temperature for 2 hours. Tubes were then centrifuged as before and the pellets were re-suspended in ice cold 70% ethanol solution before being centrifuged at 14,000 RPM for 10 min at 4^{o}C. The supernatant was discarded and the pellets dried using a vacuum centrifuge at 30^{o}C for approximately 10mins. Pellets were then re-suspended in 20 µl T-low E solution (10 mM Tris-HCl, 0.1 mM EDTA pH8) and incubated at 30^{o}C for 20 min with agitation. Samples had DNA contents evaluated using a Nanodrop (Thermo scientific) UV assay set up and stored at -80^{o}C.

Extracted samples were then subject to PCR amplification of 16S rRNA sequences using barcoded primer sets, again, as detailed in **Herbold *et al.* 2015**. The same PCR master mix was used as here previously and the cyclers were set up as follows. Twenty-five cycles of; 95^{o}C for 3 min, 95^{o}C for 30 s, 55^{o}C for 30 s,

72^{o}C for 1 min with a final single step of 72^{o}C for 7 min. From the resulting product 2 µl are added to an 18 µl volume of the second master mix containing individual barcoded-primers for each sample. The PCR ran as follows: 5 cycles of; 95^{o}C for 3 min, 95^{o}C for 30 s, 52^{o}C for 30 s, and 72^{o}C for 1 min with a final single step of 72^{o}C for 7 min. Samples were then evaluated using a Pico- green assay (Thermo Fischer) before being pooled and sent for sequencing (MiSeq).

One µl of sample was added to 99 µl of Tris/EDTA (TE) buffer and to this 100 µl of TE/Pico-green solution was added. A DNA standard was also produced with Pico-green solution and the plates were measured for absorbance at 260 nm in a plate reader. Using the standard DNA curve produced concentrations of samples were calculated and then 20 x 10^{9} amplicons per sample were pooled together for sequencing.

Results

Immuno-histology staining and spatial organisation of Muc2 Mucin

Methacarn fixation and laser micro-dissection

FISH probing of methacarn fixed samples proved difficult and sub-optimal. Bacteria were very weakly, if at all stained by the probe, as well as giving a high amount of background signal, particularly in the luminal contents. DAPI staining of host cells was successful but again gave low intensity signals for bacteria. The reason for this may be due to the LMD microscope used for micro-dissections. The LMD microscope used is only in possession of an air objective, this in combination with the Fluos fluorophore, which is often bleached rapidly in air, meant the FISH stains were not optimal. This was a recurring problem in working with the LMD as FISH images are best visible using CLSM microscopy, however can only be micro-dissected using the LMD.

Muc2 (Cy3) staining was highly successful and on that basis sections were dissected without FISH signals using the Muc2 stain as a guide. Captured micro- dissects were extracted and underwent PCR amplification.

DNA extraction and PCR

PCR recovery of genetic material from methacarn-fixed samples was evaluated using band intensity and/or presence of a band using agarose gel electrophoresis, Figure 8.

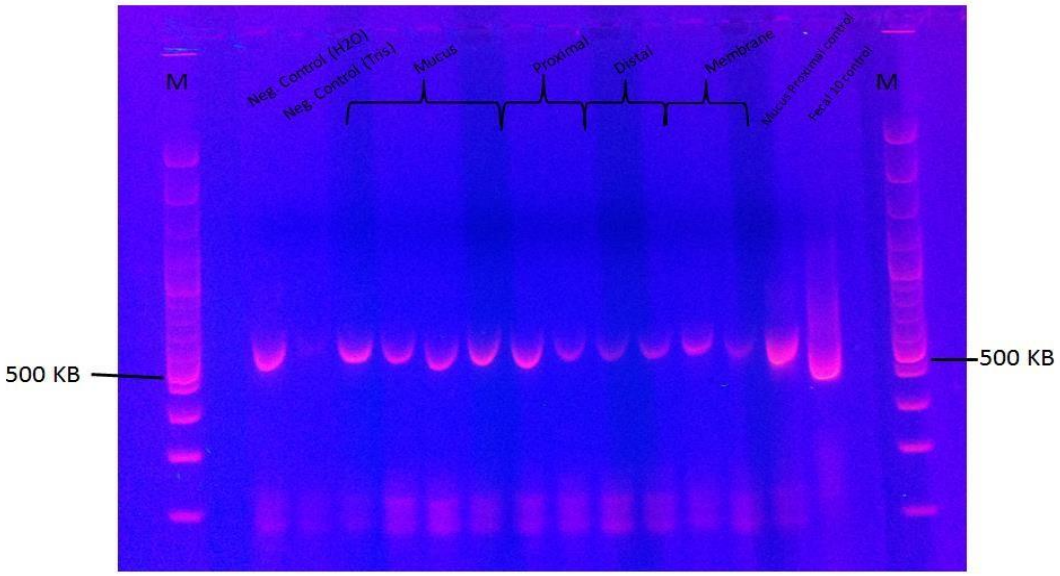

Figure 8. 1.5%Agarose gel (gel red stain) of 2 step PCR amplification of LMD-isolated, methacarn-fixed areas via Laser micro dissection. M; 1 kb DNA ladder. Negative controls had either water or Tris buffer added to the PCR reaction instead of sample. Mucus; mucus layer sections. Proximal; Sections encompassing the mucus layer and the luminal contents. Distal; sections of the luminal content. Membrane; membrane section from outside the section. Mucus proximal and faecal 10 were positive controls added to the PCR mixture in lieu of samples.

As a result of this and subsequent PCR gels showing signals in negative water controls and empty membrane dissects a more stringent PCR procedure was developed using guidelines taken from **Champlot *et al* 2010**. To combat contamination, several steps were employed to subsequent PCRs. A UV cross- linker and DNase treatment on some reagents were tried in order to eliminate potential DNA contaminations in PCR reagents. These methods allowed some removal of contaminants (Figure 9) and as a result it was decided to sequence contaminant PCR products in the future in order to identify contaminants and remove them *in silico* from sample reads. Sequencing of contaminations will allow us to eliminate those reads from the sample sequences.

Figure 9. 16S rRNA amplicons run on a 1% agarose gel (gel red stain) after decontamination steps were taken to remove artificially added contaminants. LMD slides are treated with UV crosslinking exposure and DNase treatment of some PCR components. “Empty” lanes are empty, i.e. without sections, areas of the slide excised into ATL buffer. “No membrane” lanes are from ATL eppendorfs loaded into the microscope but without any section dissected into them. “Empty new slide” lanes refer to LMD slides that were no treated with UV cross linkers beforehand. Fec2, is the positive control and contains 2 ng of genetic material taken from faecal samples.

dithiobis(succinimidyl propionate)(DSP) as a fixative for FISH protocols

Fluorescence in situ hybridisation comparison of PFA and DSP fixation on faecal homogenates

CLSM visualised slides of homogenised faecal pellets fixed in DSP or PFA were evaluated using the Leica “LAS AF” programme and further analysed using DAIME. Example images taken are shown in Figure 10.

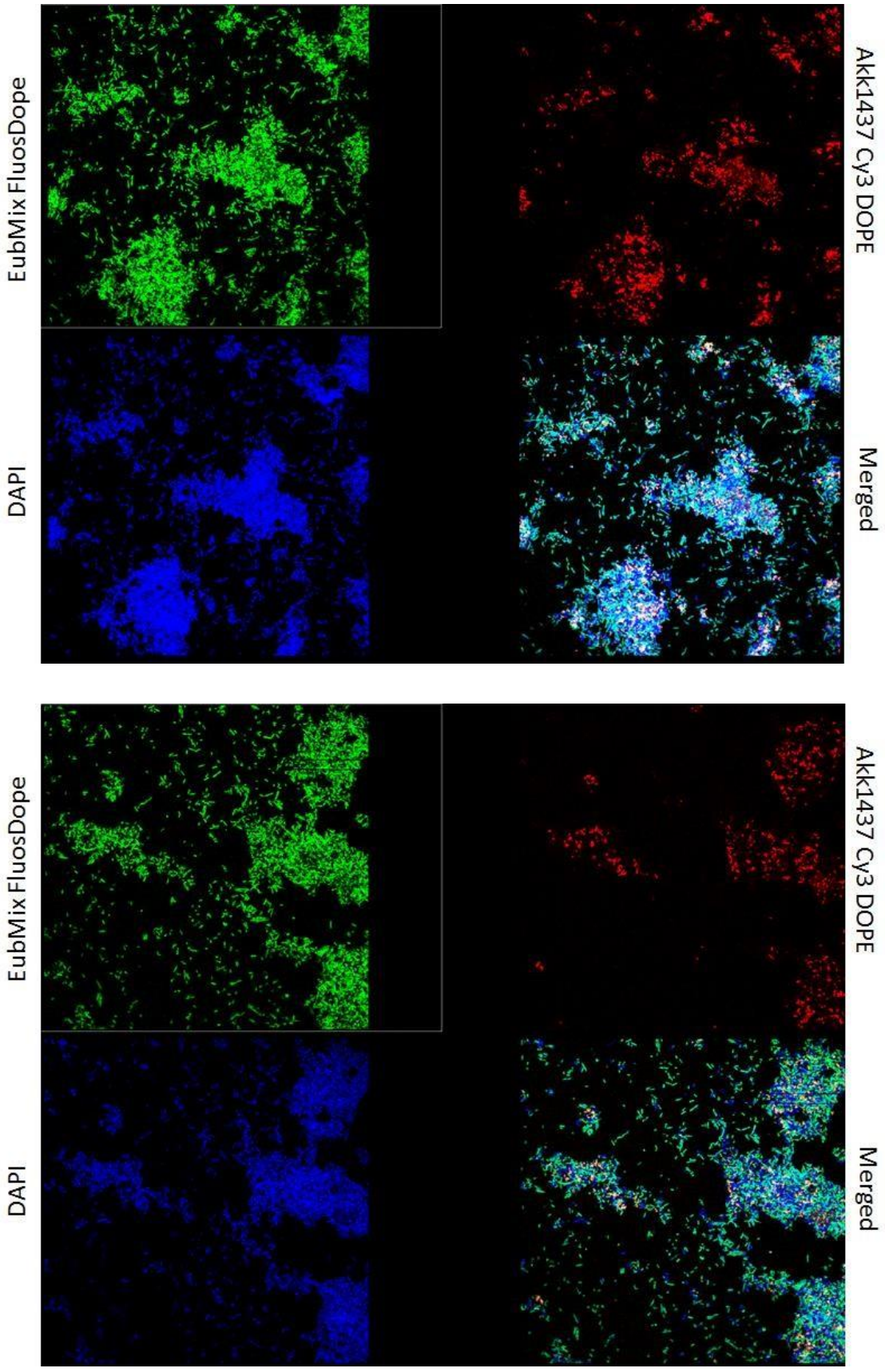
EubMix FluosDope
Akk1437 Cy3 DOPE
DAPI
Merged
EubMix FluosDope
Akk1437 Cy3 DOPE
DAPI
Merged

Figure 10. Upper 4 panels: PFA fixed samples hybridised with EUB338 I-III mix in Fluos DOPE (green), *Akkermansia* 1437 Cy3 DOPE (red) and DAPI (blue), visualised in their separate channels and also merged where indicated. Lower four panels: The same channels used to visualise DSP fixed samples.

CLSM visualised slides of homogenised faecal pellets fixed in DSP or PFA were evaluated using the Leica "LAS AF" programme and further analysed using DAIME.

These images were then subject to DAIME analysis, which compares the coverage of FISH probes and calculates the population stained in comparison to the total DAPI stained population, Figure 11.

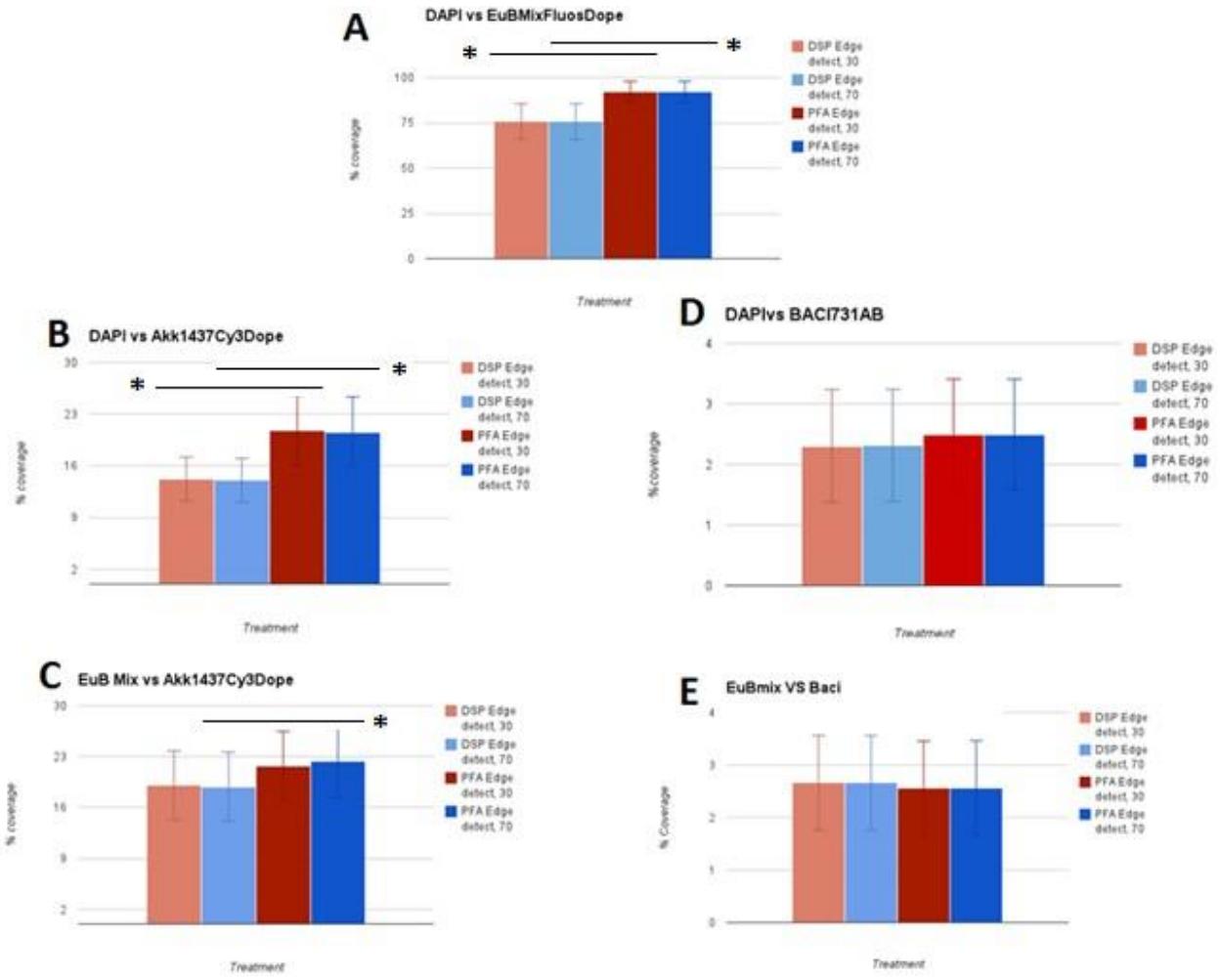

Figure 11. Results of DAIME analysis of CLSM visualised FISH stained samples show comparable population estimates. Panel A: the cumulative (20 images) percentage of cells stained with the *EUB* 338 I-III as a percentage of DAPI stained cells (i.e. total bacteria in sample). Each image set is analysed twice using a feature of DAIME that estimates objects in the sample based on background and signal intensity. Shown for both DSP and PFA fixed samples are the results obtained after analysis with DAIME using either 30% or 70% edge detection- see legend. B & D: the same analysis comparing the number of *Akkermansia* (Akk 1437 cy3 Dope) or Baci731AB stained cells as a percentage of DAPI stained cells. C&E: The same analysis comparing the number of *Akkermansia* or BACI 731AB cells as a percentage of *Eubacterium* I, II and III stained cells. All error bars are standard deviations of percentage coverage in each evaluated image group. P-values were obtained using a 2-tailed student T- Test comparing each

edge detection evaluation (30% or 70% for both DSP and PFA fixation, P-values smaller than 0.05 were considered significant and are shown as bars.

Individual signal intensities were also evaluated as FISH probes yielding lower intensities may result in under-estimates of microbial loads as some signals will fall below intensity thresholds and would therefore not be included in bio volume statistics. The signal intensities of each FISH probe and DAPI are shown in Figure 12 for each fixation treatment.

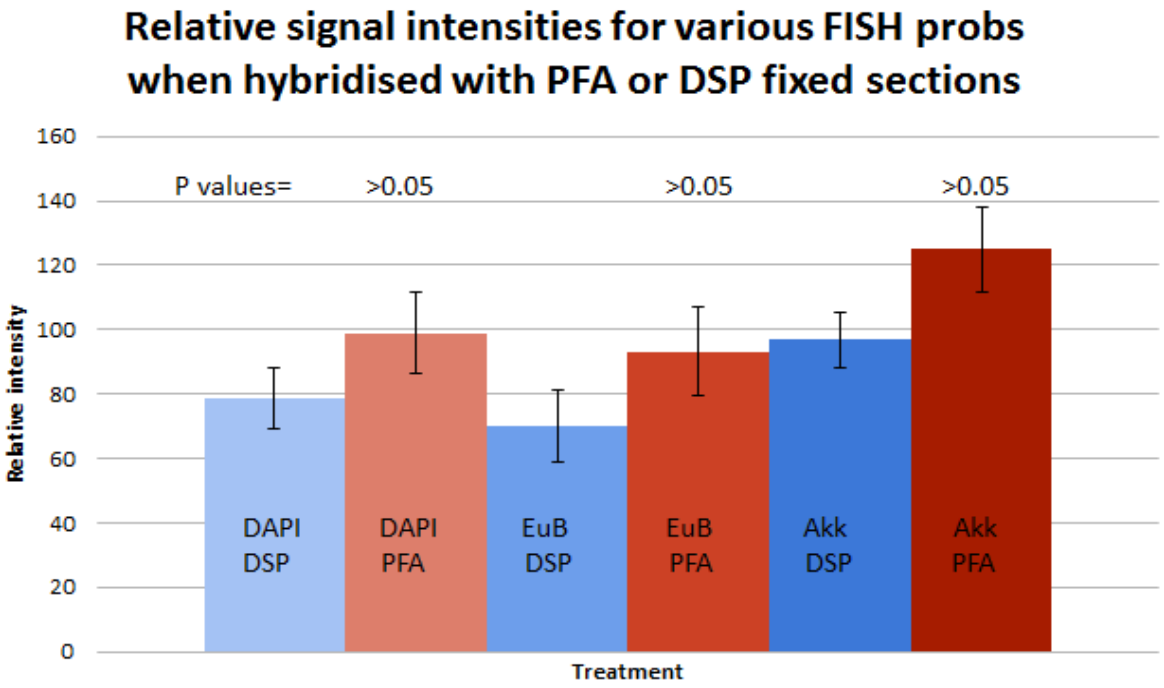

Figure 12: Relative signal intensities of individual cells in images of FISH hybridised faecal homogenates for each fixative and each FISH probe, and DAPI. DAIME software is able to evaluate the relative signal intensity per cell in an image allowing comparison of signal strength in each treatment arm. P-values are calculated using signal relative intensities for each probe compared between fixatives used. PFA gave statistically significant intensity increases compared to each DSP probe.

Immune-histology staining of Muc2 on DSP fixed colonic sections

Based on results in Figures 11 and 10, the ability of DSP as a fixative to give comparable FISH results was confirmed to an extent. We also tested whether DSP fixed sections could be successfully immune-histology stained as is the case with methacarn fixation or PFA. Muc2 was stained with anti-Muc2 antibodies and then with anti-anti bodies containing a Cy3 fluorophore and imaged on a CLSM set-up, Figure 13

A

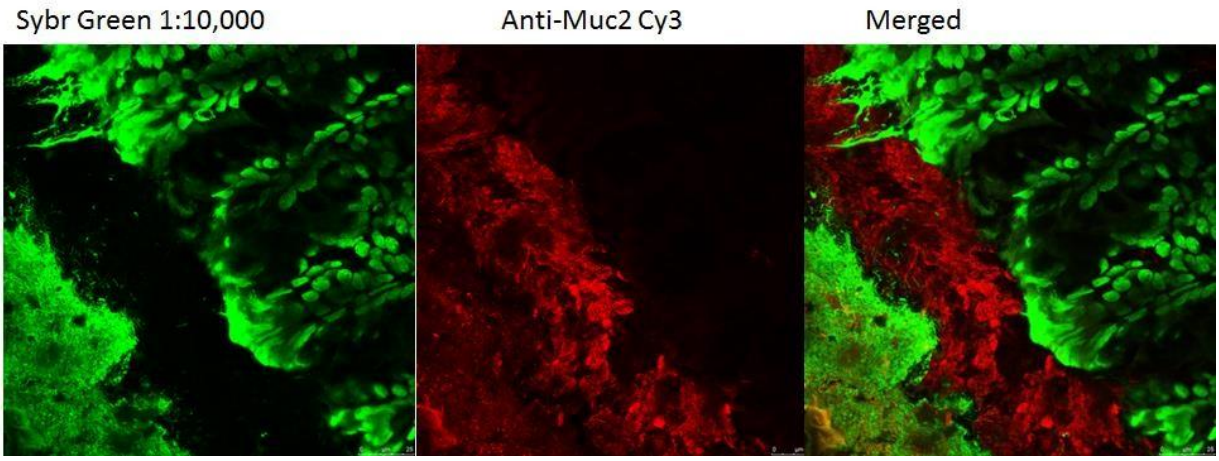

B

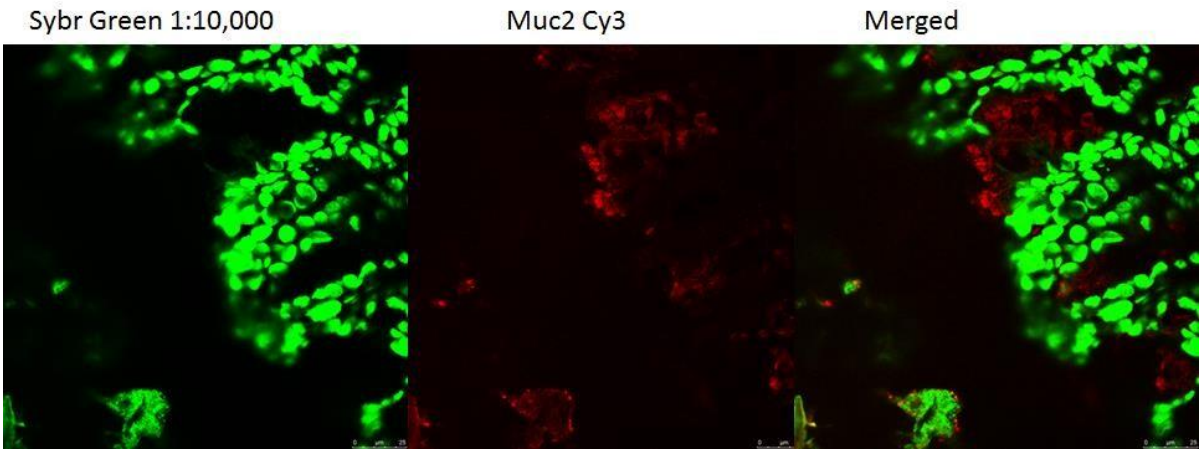

C

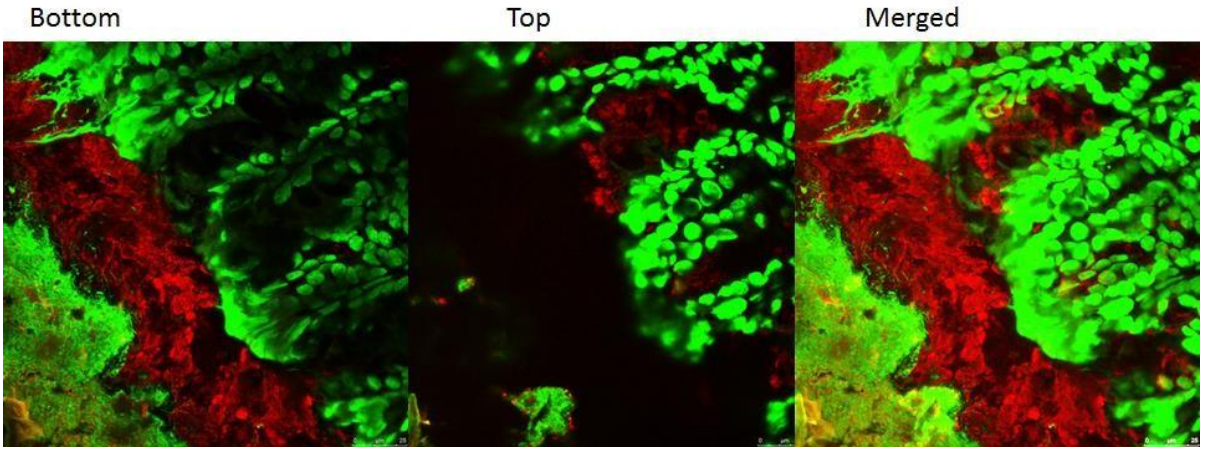

Figure 13. Immuno-histology staining of 16 µm thick mouse colonic sections visualised on a CLSM set-up (Leica). Panel A left to right: Sybr green DNA stain (1:10,000 dilution in MilliQ water, Muc2 antibody stain Cy3, merged channels. Images taken in a low Z-plane showing the Mucus boundary between the luminal contents and Epithelia. Panel B: The same channels at the same X-Y position but form an elevated Z-plane (nearer the top of the section) showing mucus accumulating in the crypts and Goblet cells. Panel C: Merged images from the top and bottom Z-planes merged together showing continuous mucus secretion from the epithelia to the lumen through the Z-plane.

Mapping Akkermansia across a fixed colon section

Due to the aforementioned difficulties in visualising FISH stained samples on an LMD microscope, we developed this protocol for FISH staining a colon section, for CLSM evaluation, and also being able to micro-dissect areas of interest. Although we were unable to use the same section for both analyses, sections were taken from the same colon and will have been under 50 µm downstream of each other. Here we attempt to compare FISH data from a PFA fixed section to the sequence data from a DSP fixed section.

The FISH stained (EuB338 I-III, *Akkermansia* and DAPI stains) section was subjected to a tile scan in which the entire section is visualised and each of the
~200 useable images were run through the DAIME software after appropriate image transformations were performed. Images containing epithelial cells were designated as the epithelial subset, and those containing no trace of epithelium were designated as the lumen subset, both sets were analysed independently and also combined.

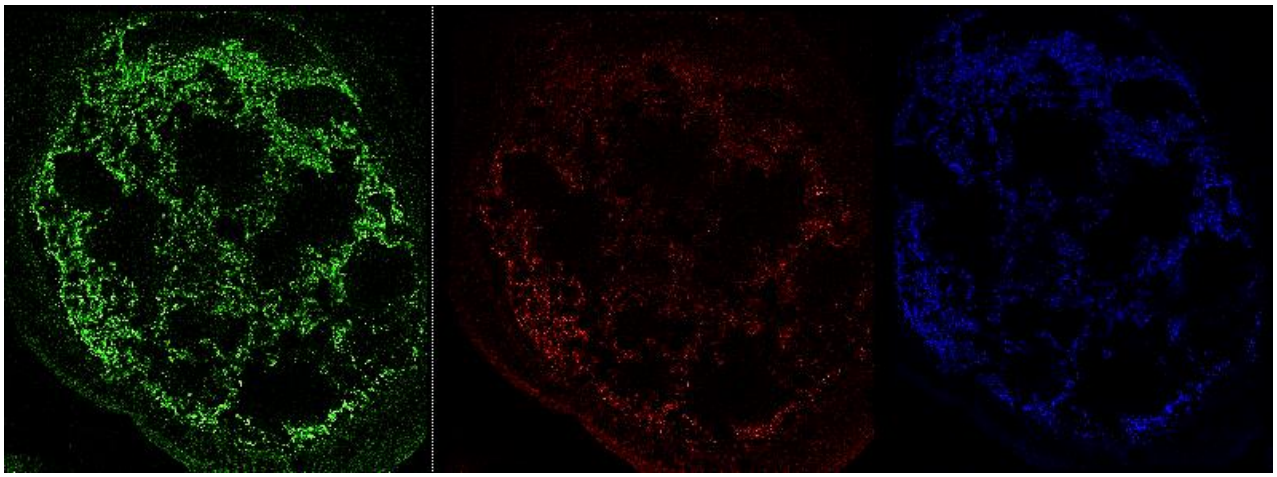

EuB I, II & III Fluos DOPE | Akk 435 Cy3 Dope | DAPI

Akk 435 Cy3 Dope | EuB I, II & III Fluos DOPE | DAPI

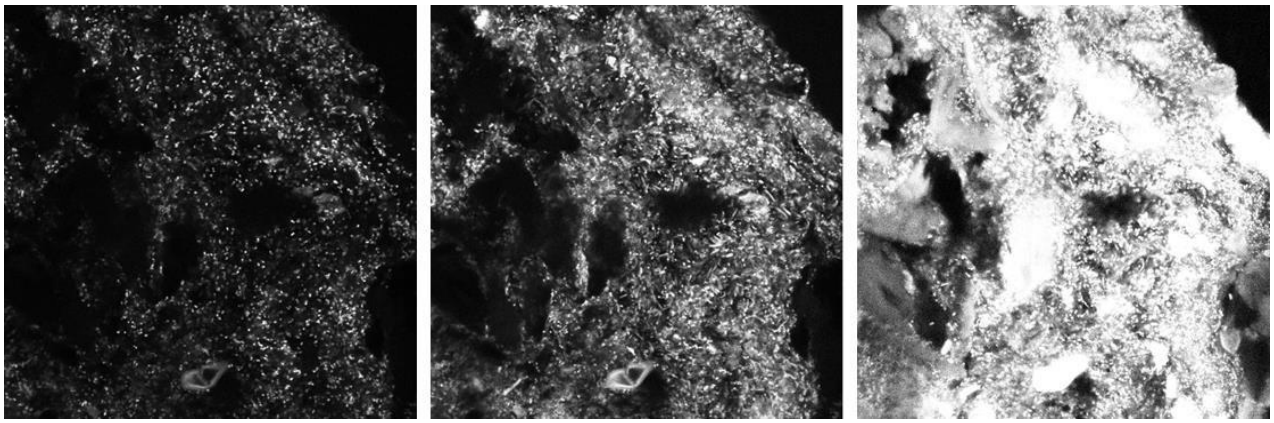

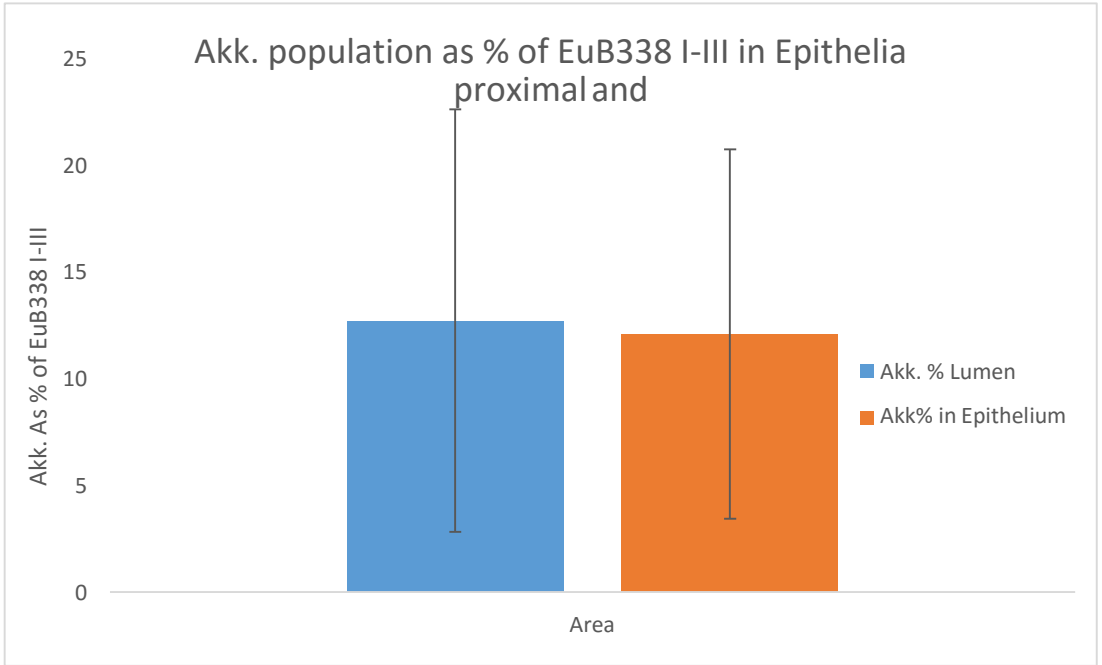

Figure 14: 3 typical FISH hybridisation images taken from a PFA fixed colon section and percentages of *Akkermansia* in each image subset. Top panel: a composite image of the entire section stained with DAPI, EuB338 I-III and Akk1437 probes, Middle Panel: a typical image from the lumen subset in the three channels used (Cy3, Fluos and DAPI). The density of signal (bacterial and auto fluorescence of digesta) in the DAPI channel meant useful image analysis was difficult using the DAPI images, therefore *Akkermansia* population percentages were calculated in comparison to the *Eubacteria* probe populations. Lower Graph: percentages of *Akkermansia* as a proportion of EuB338 I-III stained species in both the epithelium subset and luminal subset. The combined average of both subsets is 12.57% (12.7% in the lumen and 12.07% in epithelial images).

The average *Akkermansia* coverage for the "lumen" and "epithelial proximal" images were 12.7% and 12.07% respectively and combined across the whole section the average was 12.5%.

Compared to these data were sequence data for micro-dissects from a single colon section from the same mouse. These sections were extracted and 16S rRNA sequences amplified and barcoded to be sequenced.

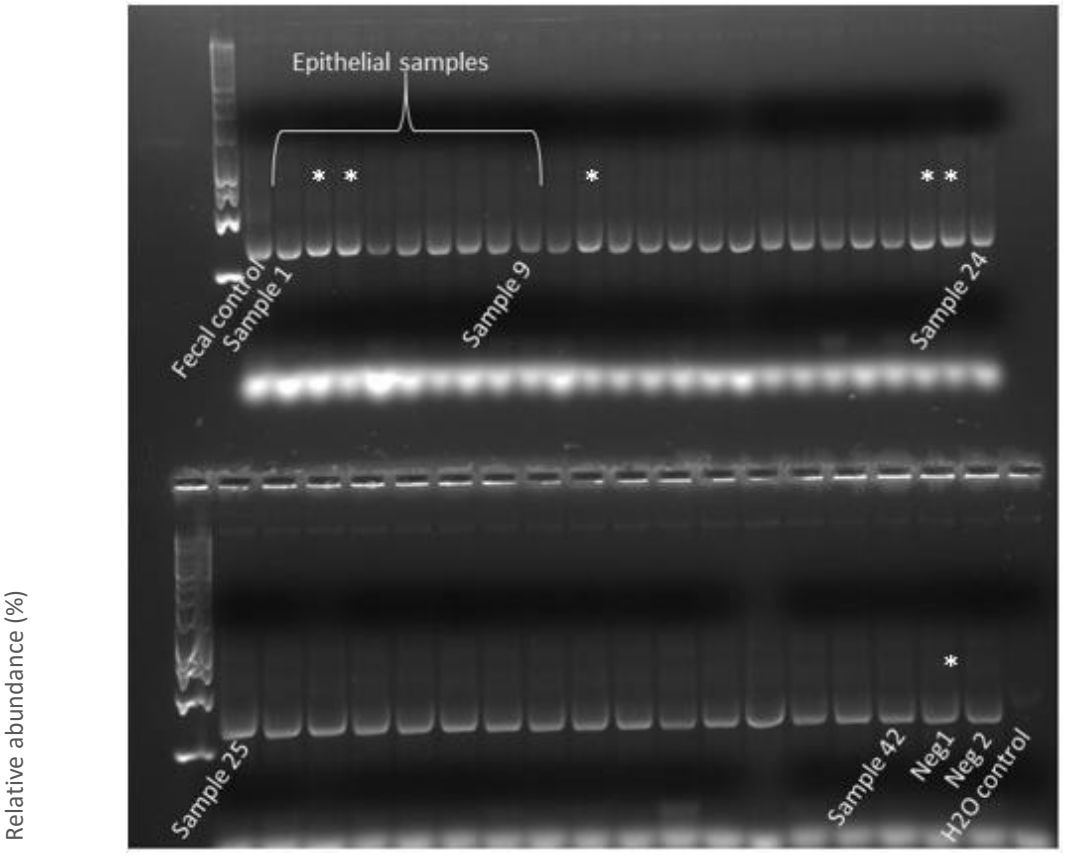

Figure 15. 1.5% agarose gel with 42 loaded samples as designated in Figure 6 after PCR amplification with general primers. Starred (*) samples were re-amplified using barcode primers, subject to PCR clean up with magnetic microbeads (Agencourt) between the two PCR steps and sent for sequencing. Faecal control is 10 µg mix of bacterial DNA used as a positive control. Samples 1-9 were exclusively micro-dissected from the epithelial area and the remaining samples from the lumen. Neg1 and Neg2 are empty LMD samples.

After sequencing of the 5 micro-dissects from the DSP fixed colon, statistical analyses were conducted. Although signal reads were detected in the PCR water control, these operational taxonomic units (OTUs) are not considered to be gut residing bacteria. One sample (sample 2 from the "epithelial proximal" designation) was shown to contain only 3 OTUs all of which were in high abundance in the water control, we would therefore suggest this sample failed during a PCR step and contains only bacteria from the water contamination. Sample 2 was therefore excluded from further statistical analysis. Taxa thought to be non-gut dwelling were also selectively excluded from the remaining sample reads. Leaving only OTUs from the *Firmicutes, Bacteroidales, Verrucomicrobia, Defferibacteres, Actinobacteria,* candidate phylum TM7, *δ Proteobacteria*, and *ε Proteobacteria.* OTUs that software were unable to place into any specific taxa were therefore also removed, the results are shown in Figure 16.

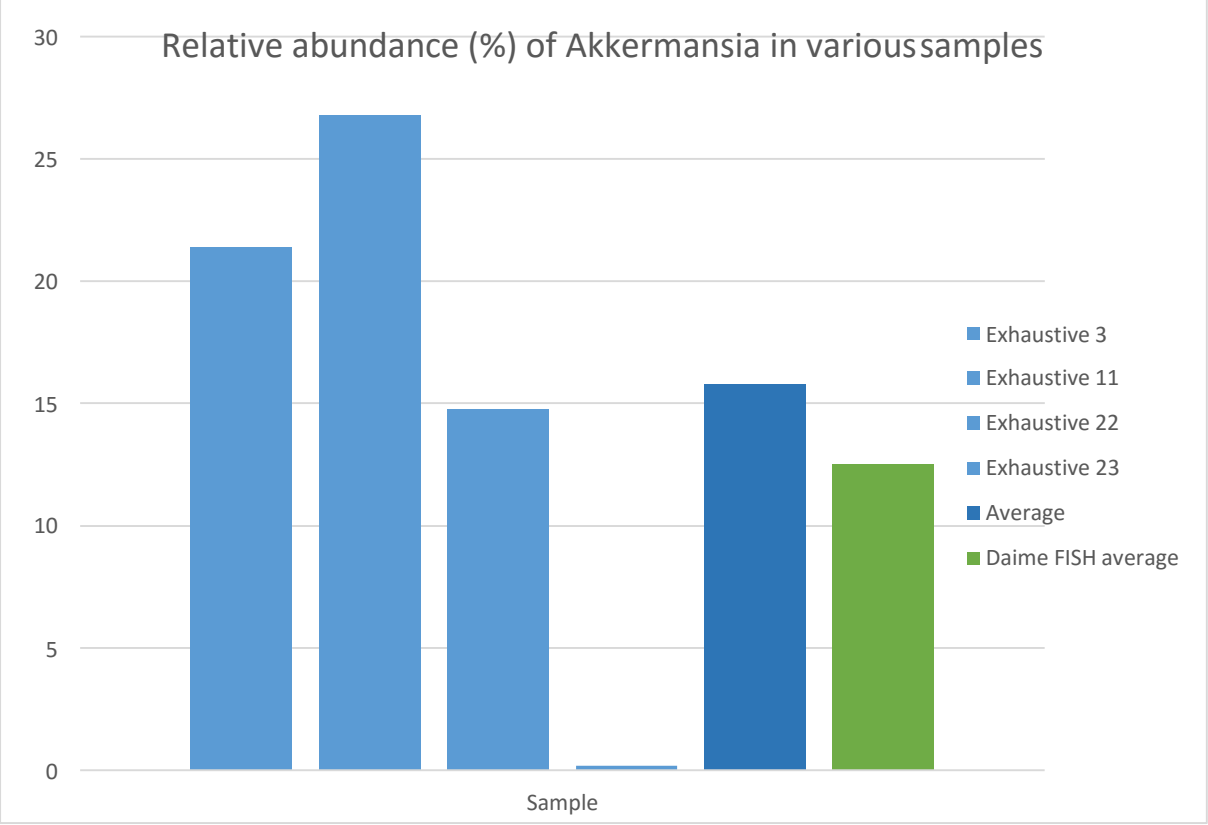

Figure 16: Graphical depiction of the relative abundance of *Akkermansia* sequences as a total of all reads after removal of known non-gut OTUs. Samples 3, 11, 22 and 23 are shown individually and also their combined average "total average". Also shown is the total average of *Akkermansia* relative abundance from the FISH analysis on a similar colon section, as seen in Figure 14 (in green).

Depicted below in Figure 17 are the number of *Akkermansia* reads from the sequencing result compared to the total number of reads from all OTUs.

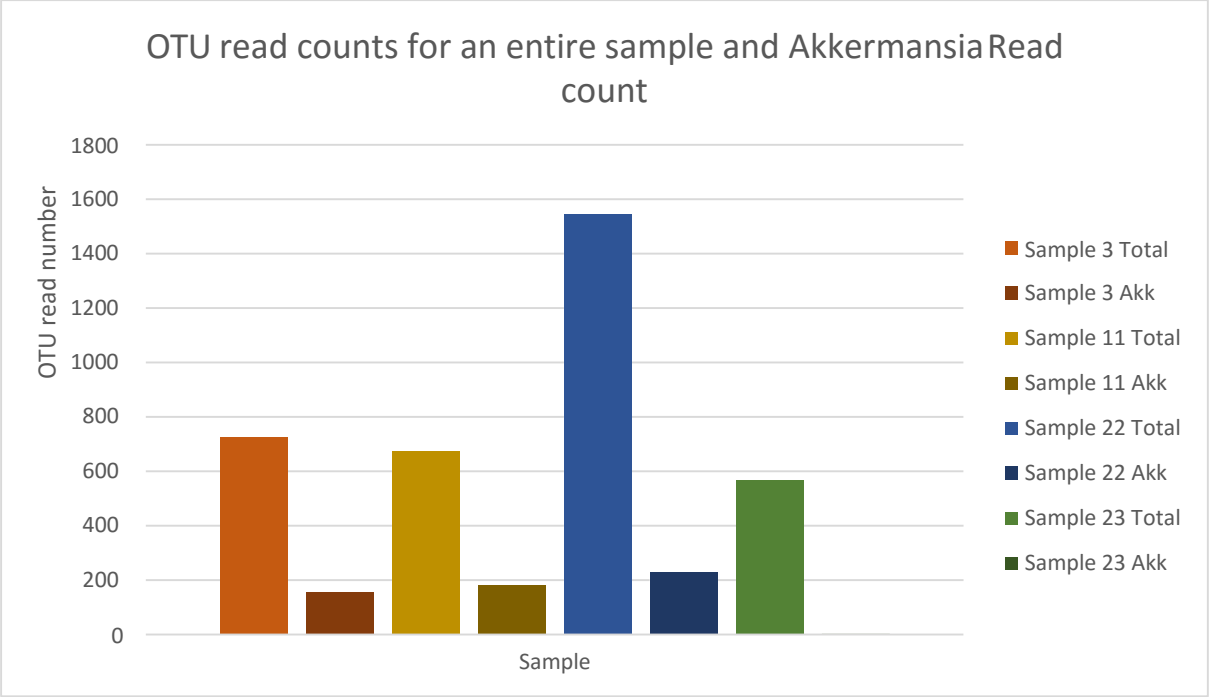

Figure 17: Total OTU reads for each sample compared to total *Akkermansia* reads per sample.

Semi-quantitative distribution of Akkermansia in colons of mice on two diets

DSP fixed mice colons on the same diet in either powder or pellet form were also subject to the same PCR amplification as above before being sent for sequencing. In this we attempted to semi-quantitatively evaluate the power of DSP fixation to yield results that reflect subtle differences in two colon sections with differing populations of *Akkermansia*.

Firstly, total counts for all OTUs were collated which may indicate a bias in the number of *Akkermansia* reads, and are shown in Figure 18.

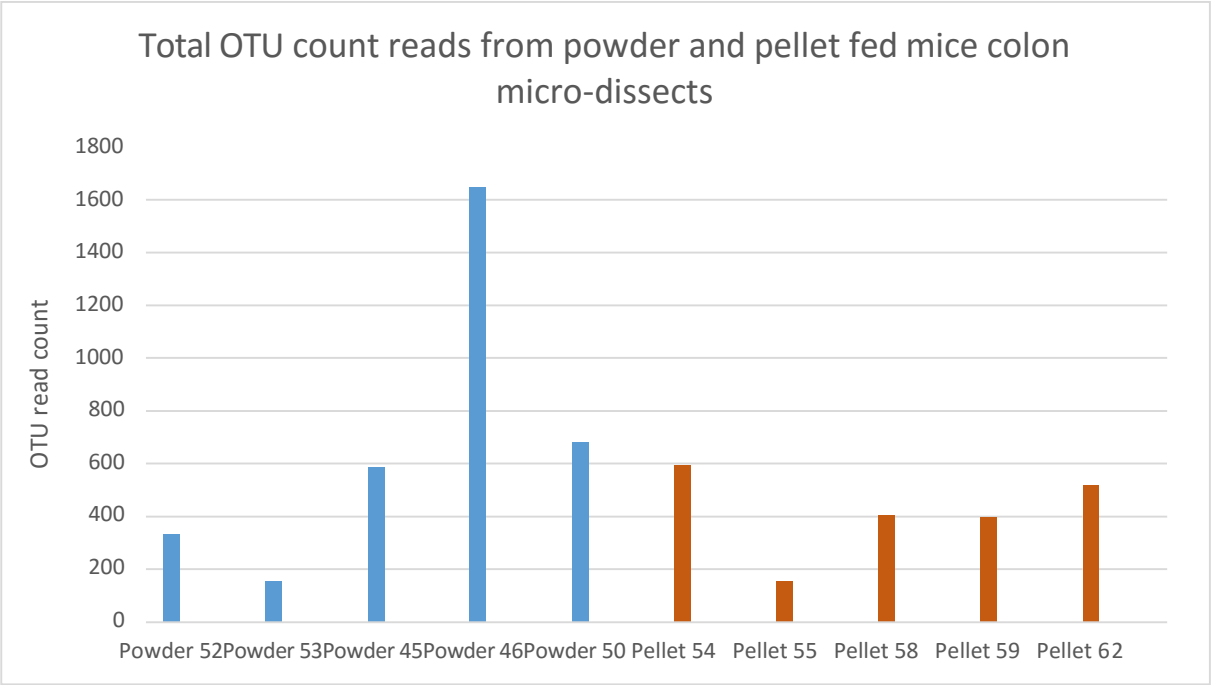

Figure 18. Total OTU counts for 5 micro-dissects from one colon section of mice fed on the normal "chow" in either pellet or powder form. No statistical difference is seen between the two experimental branches after a Student's T-test.

The total *Akkermansia* OTUs were then evaluated as a percentage of each micro-dissect sample and are summarised in Figure 19.

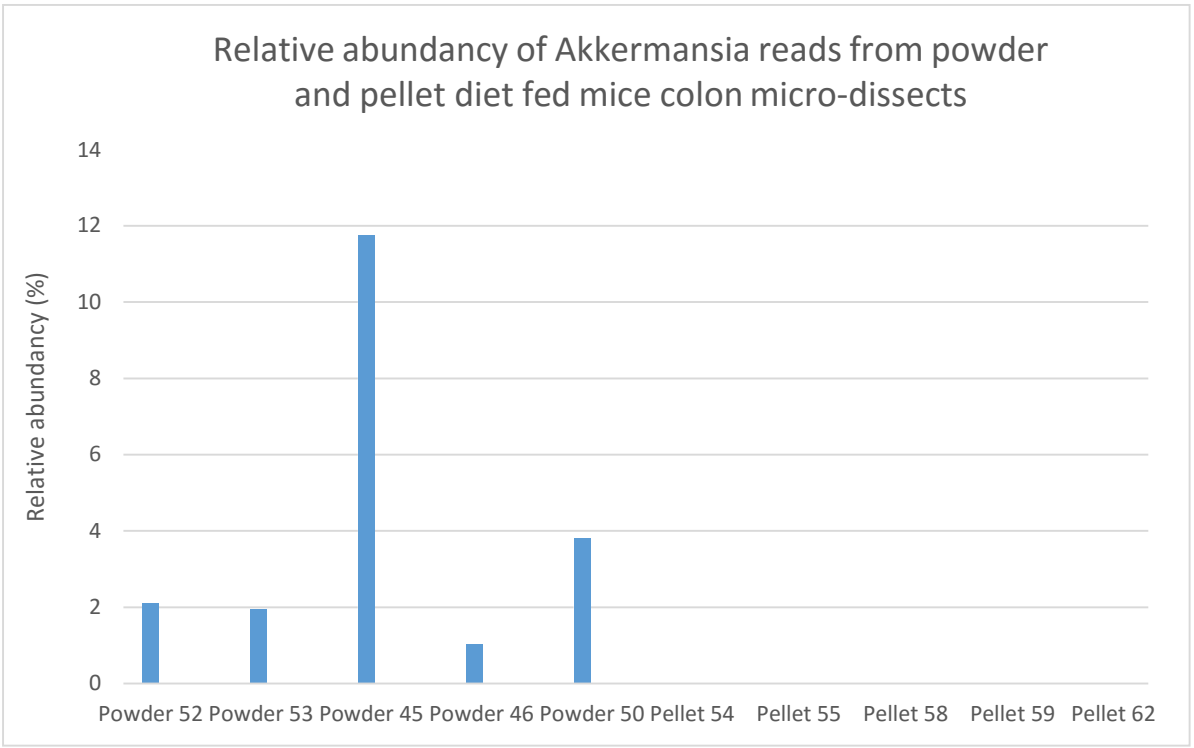

Figure 19. Relative abundancies of *Akkermansia* OTU as a percentage of total OTU counts shown in Figure 18. Pellet diet sequence results consistently showed no trace of *Akkermansia* reads.

Sequence data from samples were analysed for relationships between samples using the R statistical software (R-project.org) with the "vegan" ecology package (**Oksanen *et al.* 2015**). The powder and pellet diet sample data were subject to a metaMDS analysis from the package ,after using a Bray-Curtis dissimilarity matrix and rarefied to the smallest sample Library and the, results are shown in Figure 20. Additionally the sample data were also analysed against sequence data from the previous experiment "*Mapping Akkermansia across a fixed colon section"* and these are shown also in Figure 20.

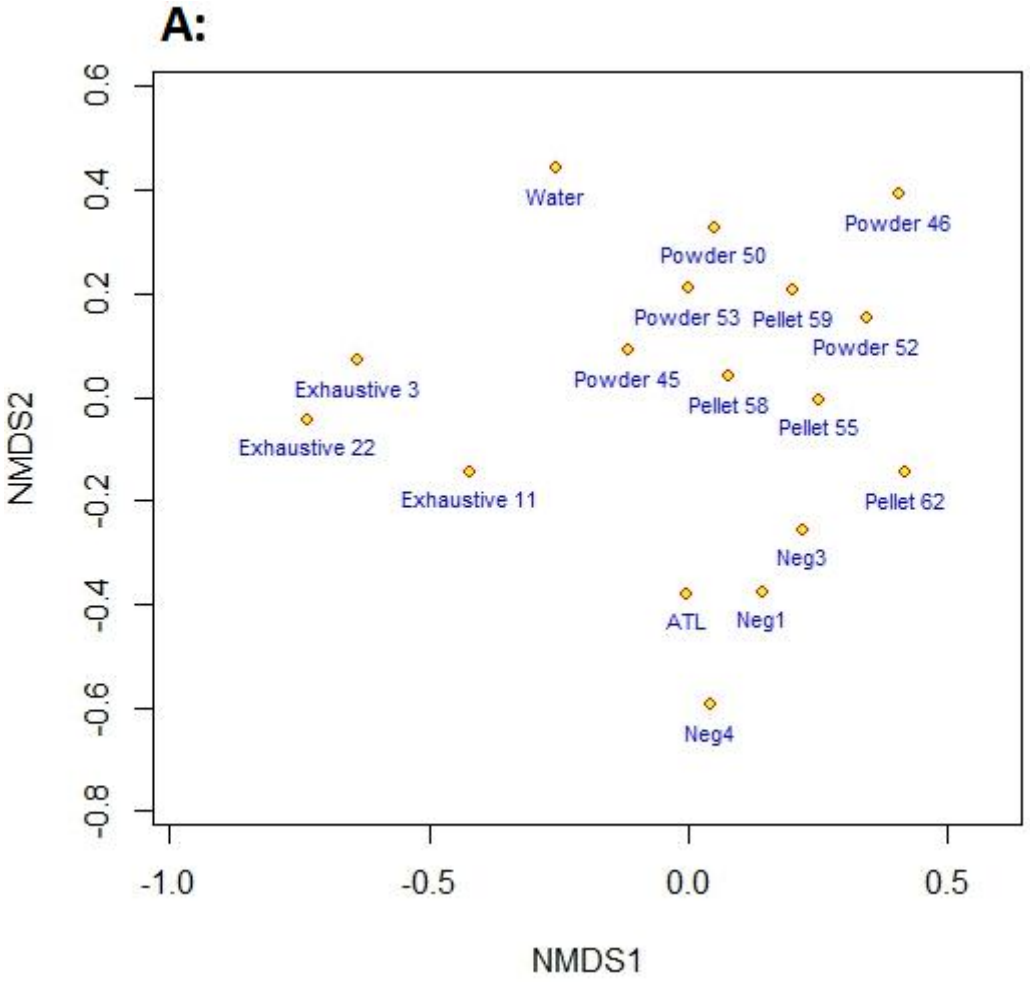

B:

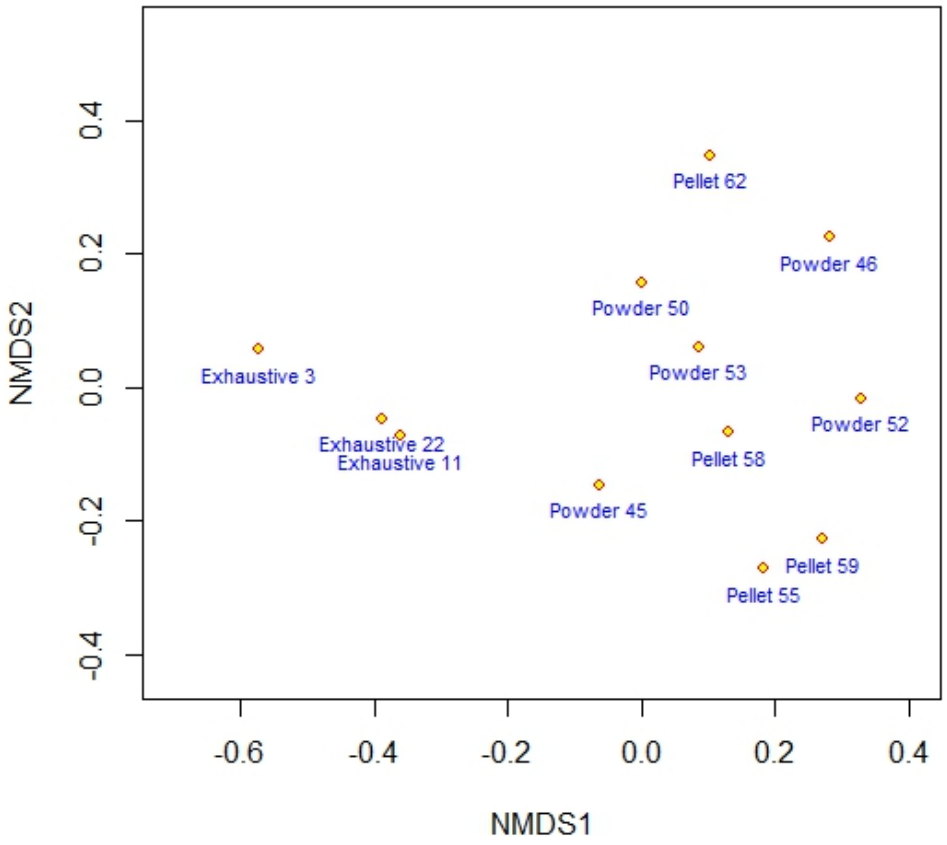
Pellet 62
Powder 46
Powder 50
Exhaustive 3
Powder 53
Powder 52
Exhaustive 22
Exhaustive 11
Pellet 58
Powder 45
Pellet 59
Pellet 55
NMDS2
NMDS1
0.4
0.2
0.0
-0.2
-0.4
-0.6
-0.4
-0.2
0.0
0.2
0.4

C:

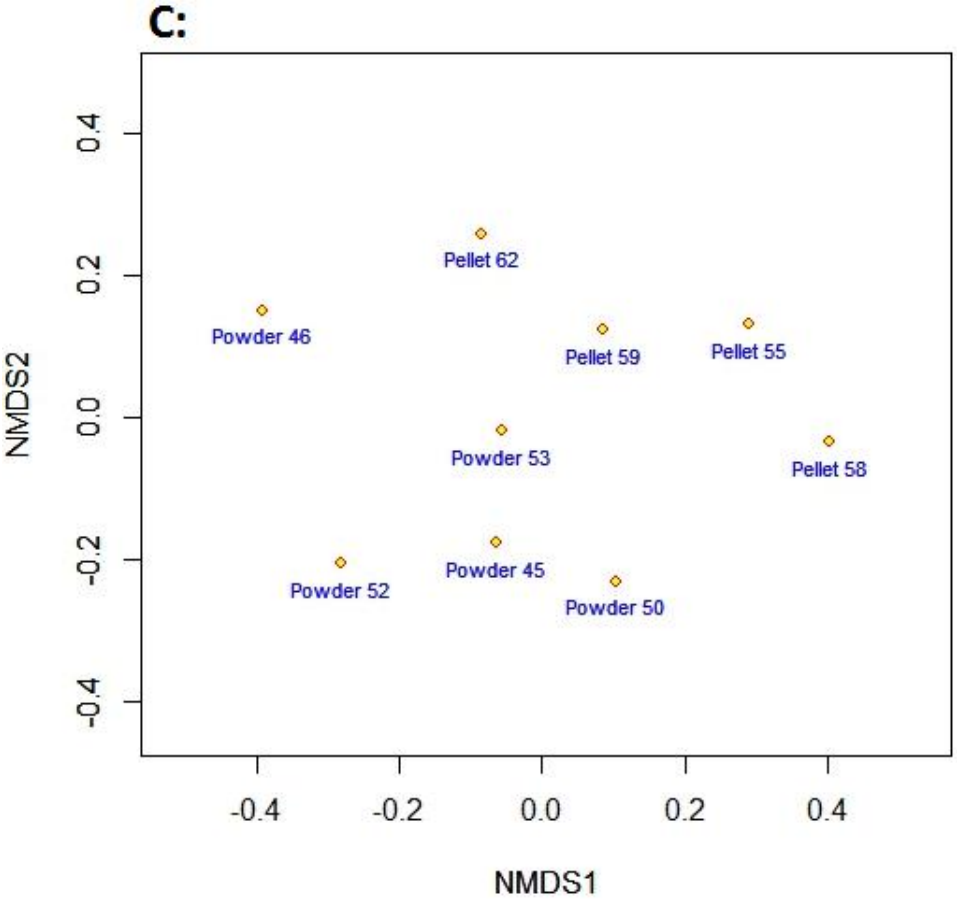
Pellet 62
Powder 46
Pellet 59
Pellet 55
Powder 53
Pellet 58
Powder 45
Powder 52
Powder 50
NMDS2
NMDS1
0.4
0.2
0.0
-0.2
-0.4
-0.4
-0.2
0.0
0.2
0.4

Figure 20. Ecological relatedness between samples based on a MetaMDS analysis after removal of non-gut residing OTUs using the "vegan" package for R (**Oksanen *et al.* 2015 and R-project.org**). A: All samples from both studies are rarefied to Water controls (100 reads). B: The same samples without the controls, rarefied to the smallest library (150 reads.). Two samples from B are excluded due to their position outside the rest of the samples ("Exhaustive 23"and "pellet 54). C: results for the powder or pellet diet treatment arms compared against each other.

FISH probe design against the* Erysipelotrichaceae *family

In silico FISH probe design

The Cy3 labelled FISH probe ALBA365 Cy3 and its unlabelled competitor cALBA365 as seen in Table 1 were ordered (Biomers, Germany) and used in subsequent evaluations of its hybridisation dynamics as detailed below.

In vitro probe evaluation

After hybridizing ALBA365 Cy3 and cALBA365 (unlabelled), at a range of formamide percentages, with cecal homogenate and staining with DAPI stain, DAIME was used to evaluate the optimal formamide concentration which gives the highest intensity of signal per stained cell. The relative abundancies of ALBA365 Cy3 as a percentage of DAPI stained total bacterial load was also evaluated and both are shown in Figure 22. The parallel hybridization including EuB338 I, II&III were conducted identically and the results are shown in Figure 23. An example of FISH images taken can be seen in Figure 21.

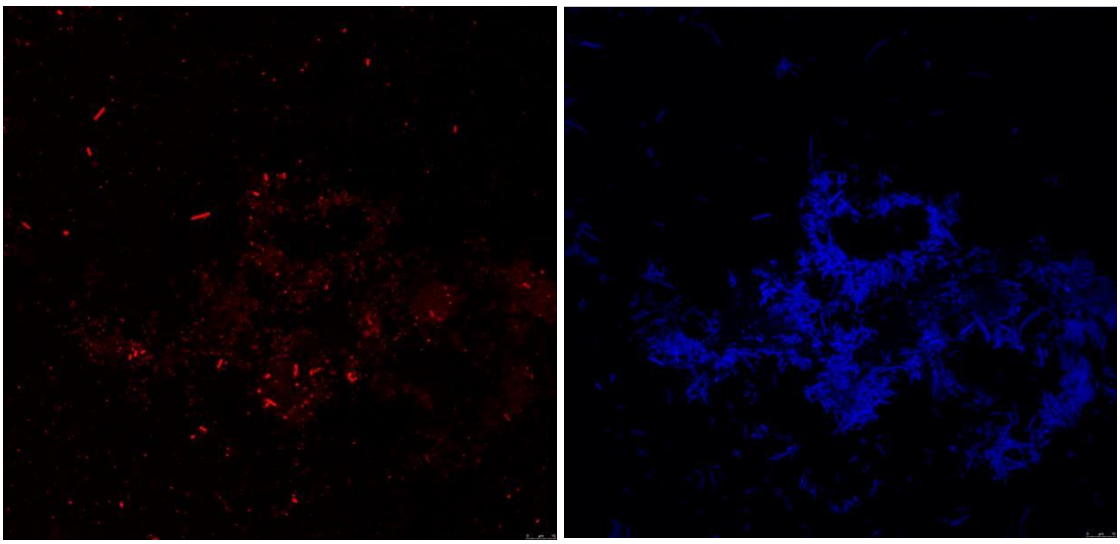

ALBA365 Cy3 DAPI

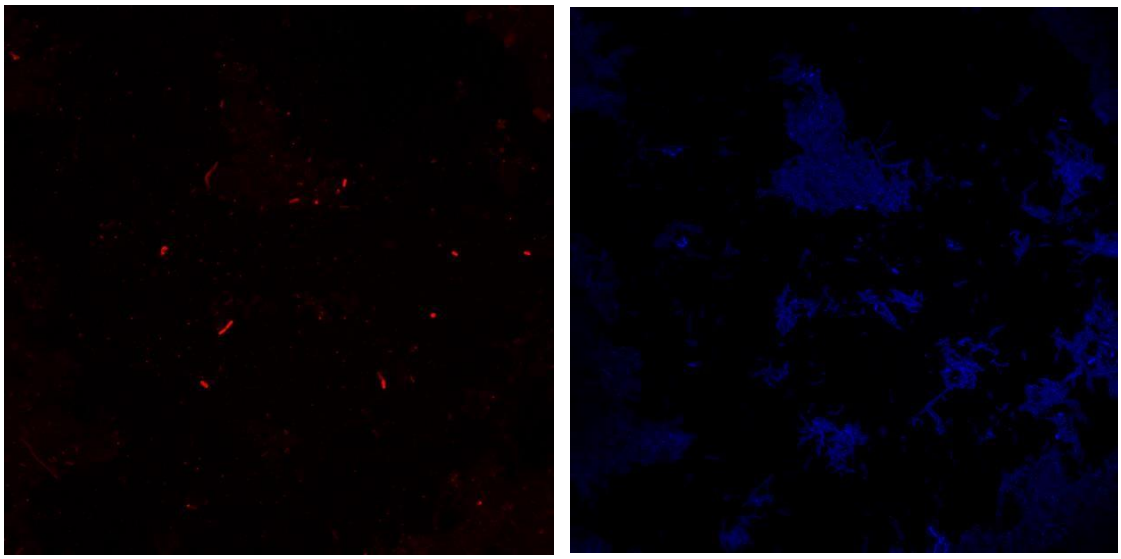

ALBA365 Cy3 DAPI

EuB 338 I, II&III Fluos Dope

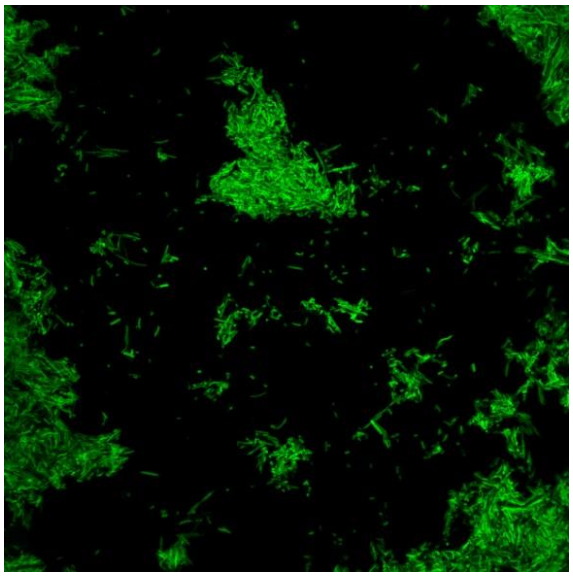

Figure 21. Example images from 0% FA hybridisations of both ALBA 365 Cy3 and cALBA365 with DAPI (top two images) and 0% FA hybridization with ALBA365 Cy3, cALBA 365 and EuB I, II&III Fluos DOPE with DAPI.

We then analysed each image set to calculate the optimal formamide concentration and also populations stained by each probe Figures 22 & 23

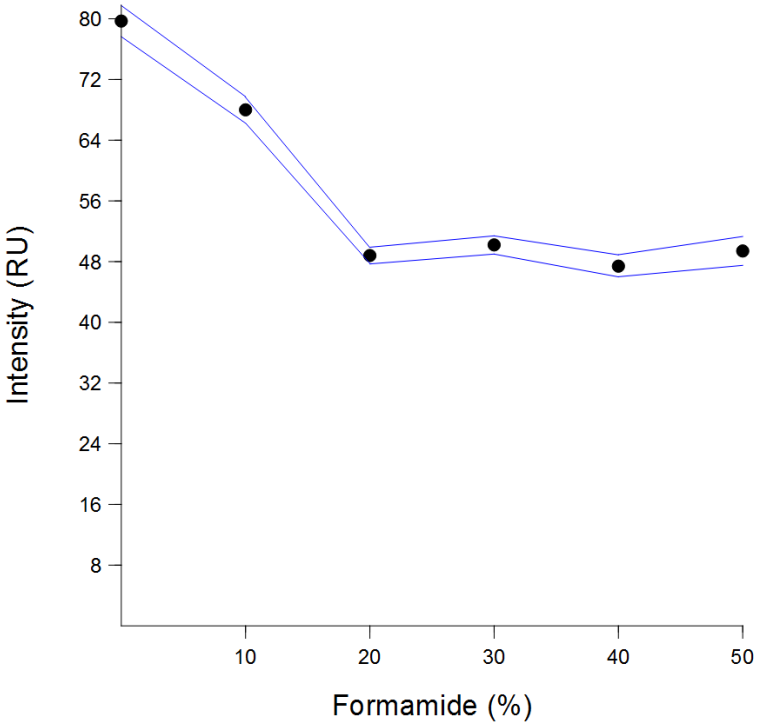

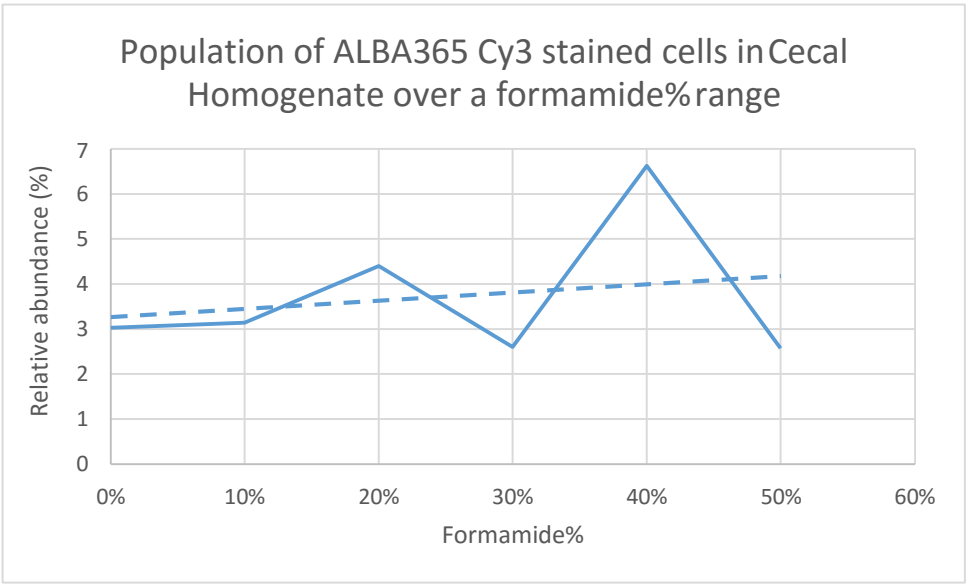

Figure 22. Results of hybridizing cecal homogenate samples with ALBA365 Cy3 and cALBA365 over a range of formamide concentrations. Upper panel: the formamide curve as calculated by DAIME to calculate the optimal formamide concentration which gives the most intense signal per stained cell. Lower panel: The relative abundance of ALBA365 stained cells as a ratio of DAPI stained cells over the same formamide concentration range showing the trend line over these concentrations (dashed line).

A

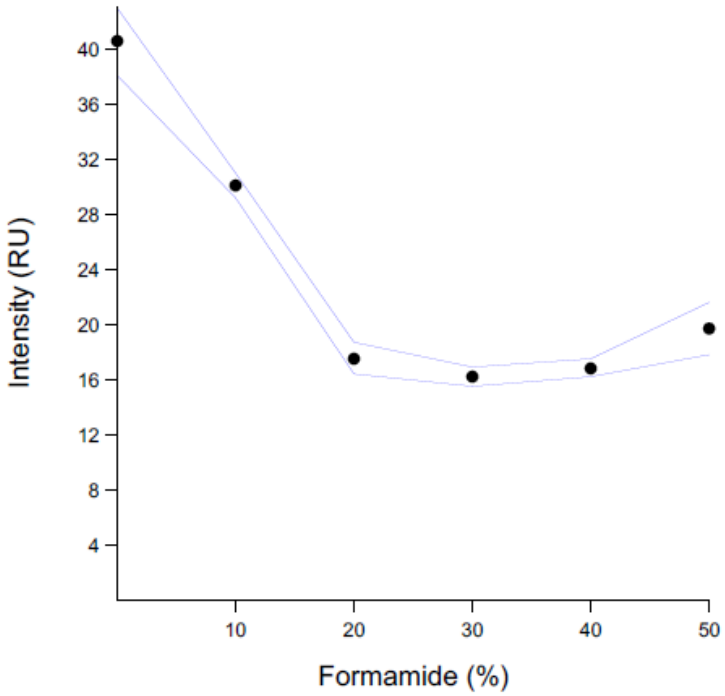

B

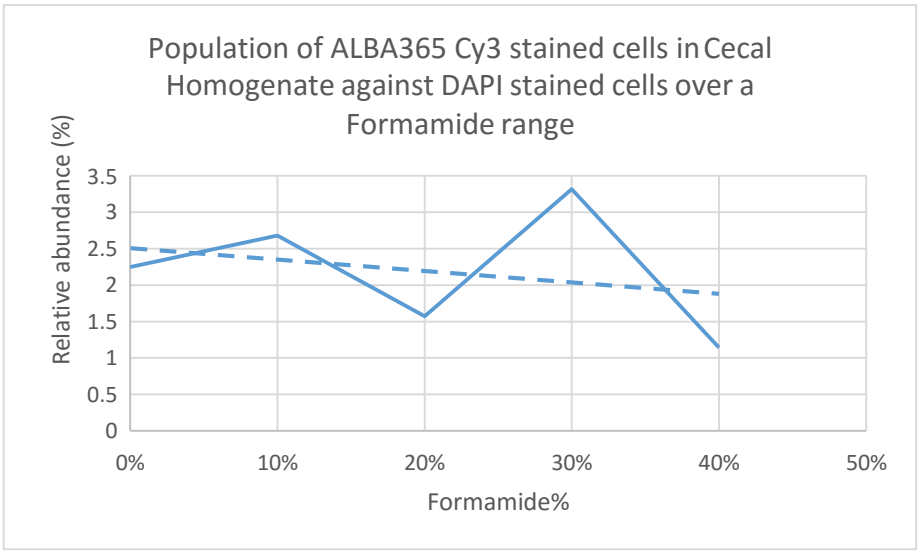

C

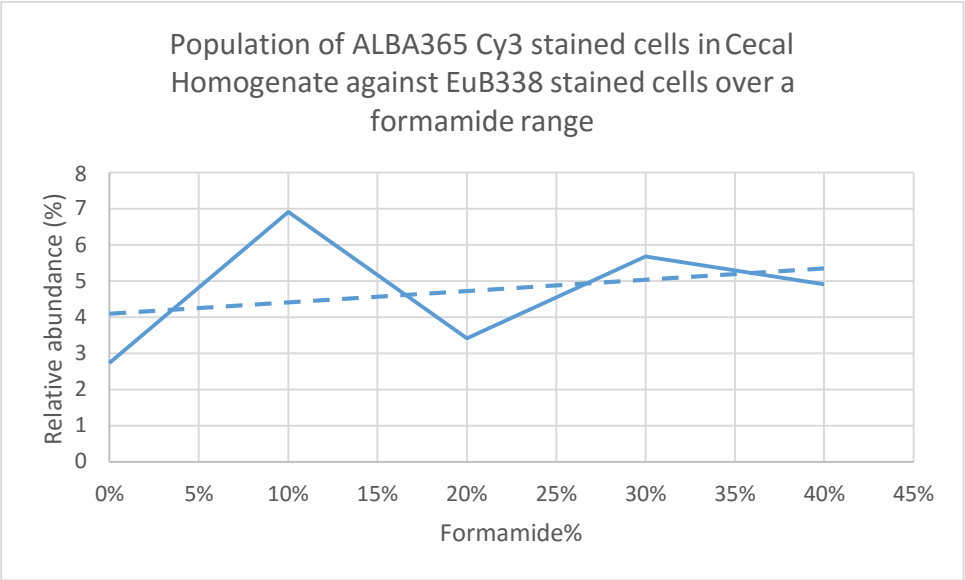

D

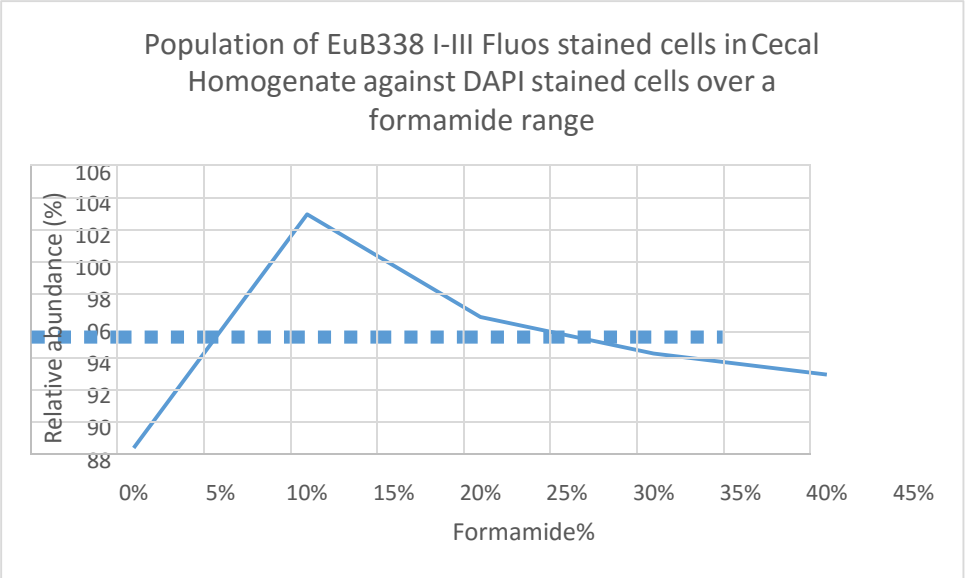

Figure 23. Results of hybridizing cecal homogenate samples with ALBA365 Cy3, EuB338 I-III Fluos and cALBA365 over a range of formamide concentrations. Panel A: the formamide curve as calculated by DAIME to calculate the optimal formamide concentration which gives the most intense signal per stained cell. Panel B: The relative abundance of ALBA365 stained cells as a ratio of DAPI stained cells over the same formamide concentration range showing the trend line (dashed) over these concentrations. Panels C and D are the populations of ALBA 365 stained cells as a proportion of 338 stained cells and EuB338 I-III 338 stained cells as a proportion of DAPI stained cells respectively.

Mucinase assay development

Free sugar release assay

Reducing sugar release was measured by the addition of DNS to sample wells after various time points of incubation with faecal homogenate and porcine stomach mucus, and subsequent measurement of 540 nm absorption. From raw 540 nm Absorption values of a maltose dilution series a standard curve was produced and the concentration of experimental samples was calculated using this standard curve. The results are shown in Figure 24 and 25.

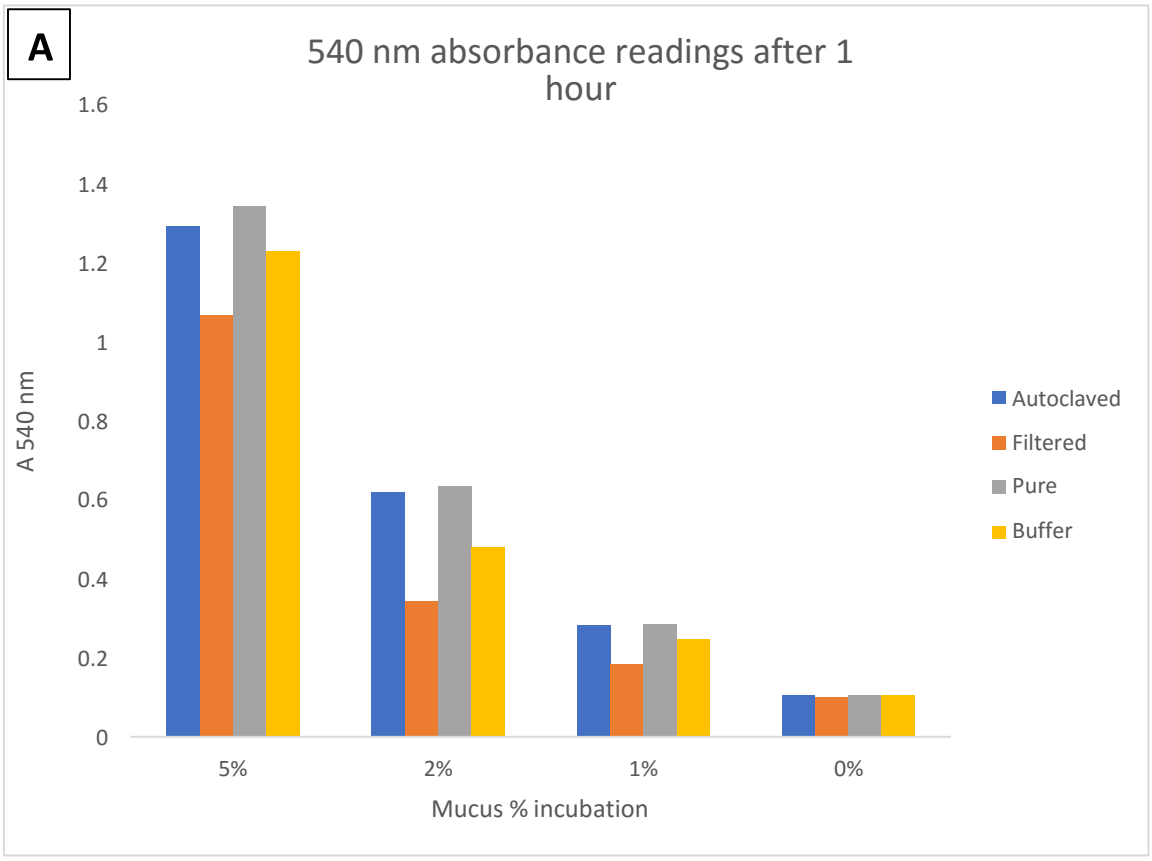

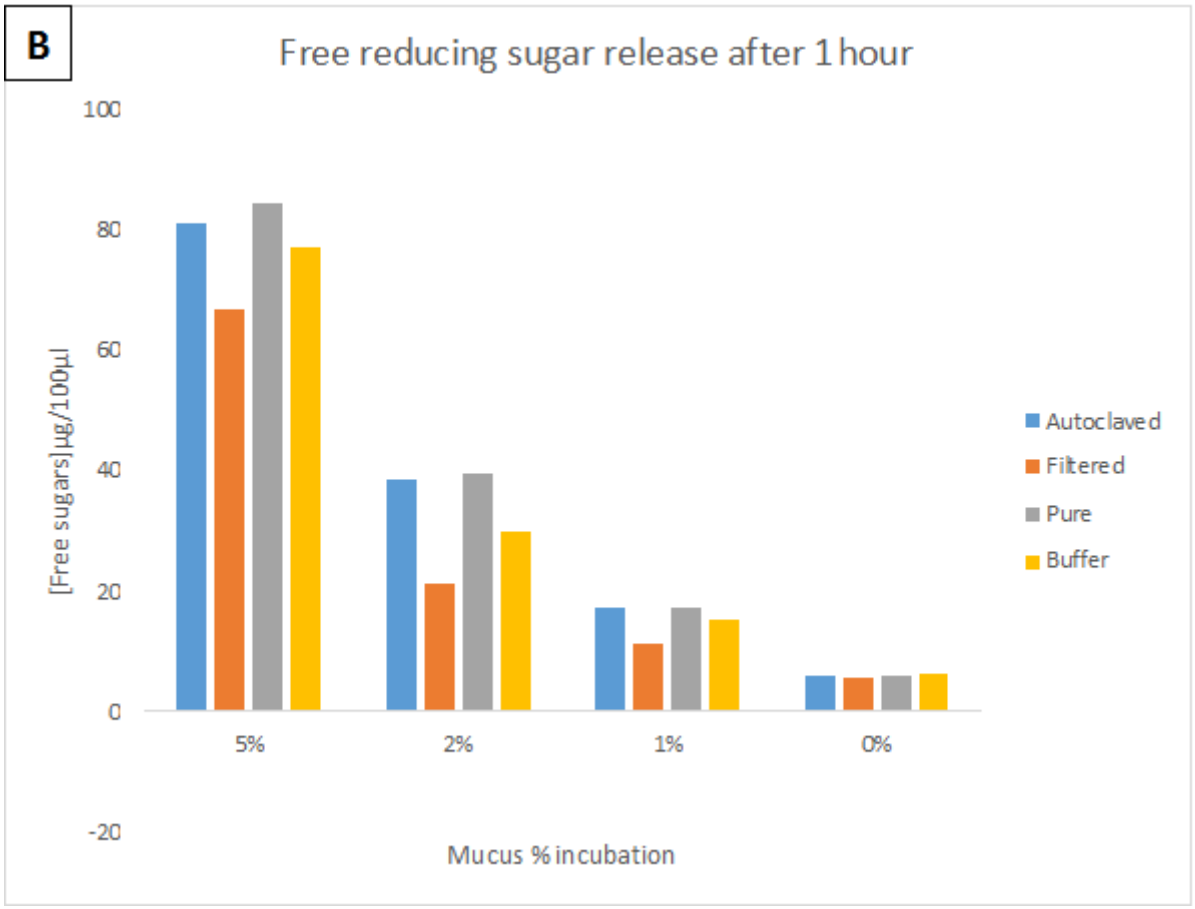
B
Free reducing sugar release after 1 hour
100
80
60
40
20
0
-20
[Free sugars] µg/100µl
5%
2%
1%
0%
Mucus % incubation
Autoclaved
Filtered
Pure
Buffer

C

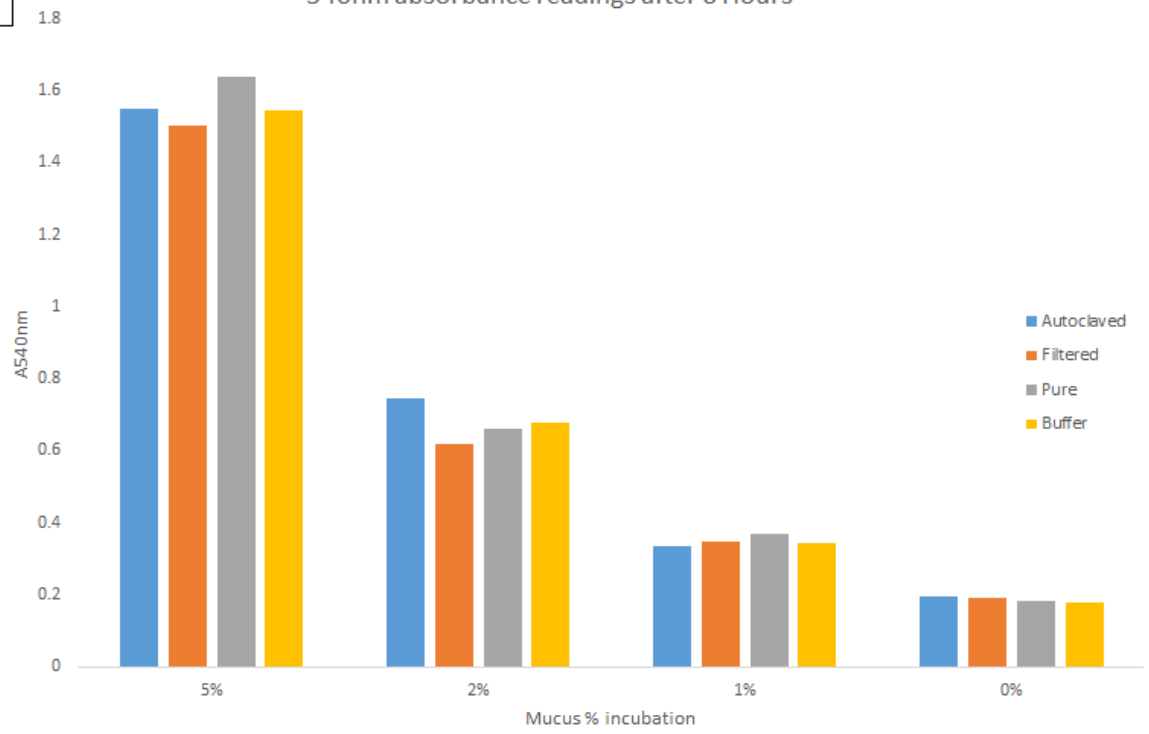
540nm absorbance readings after 6 Hours
A540nm
1.8
1.6
1.4
1.2
1
0.8
0.6
0.4
0.2
0
5%
2%
1%
0%
Mucus % incubation
Autoclaved
Filtered
Pure
Buffer

D

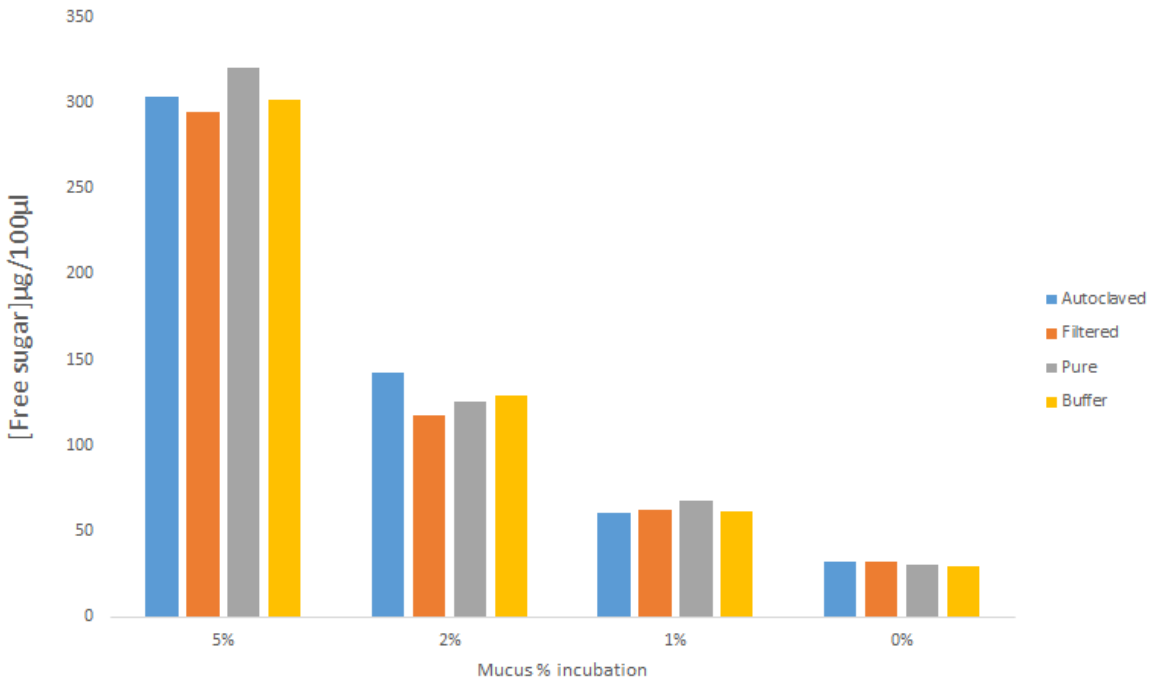
Free reducing sugar release after 6 Hours
[Free sugar]µg/100µl
350
300
250
200
150
100
50
0
5%
2%
1%
0%
Mucus % incubation
Autoclaved
Filtered
Pure
Buffer

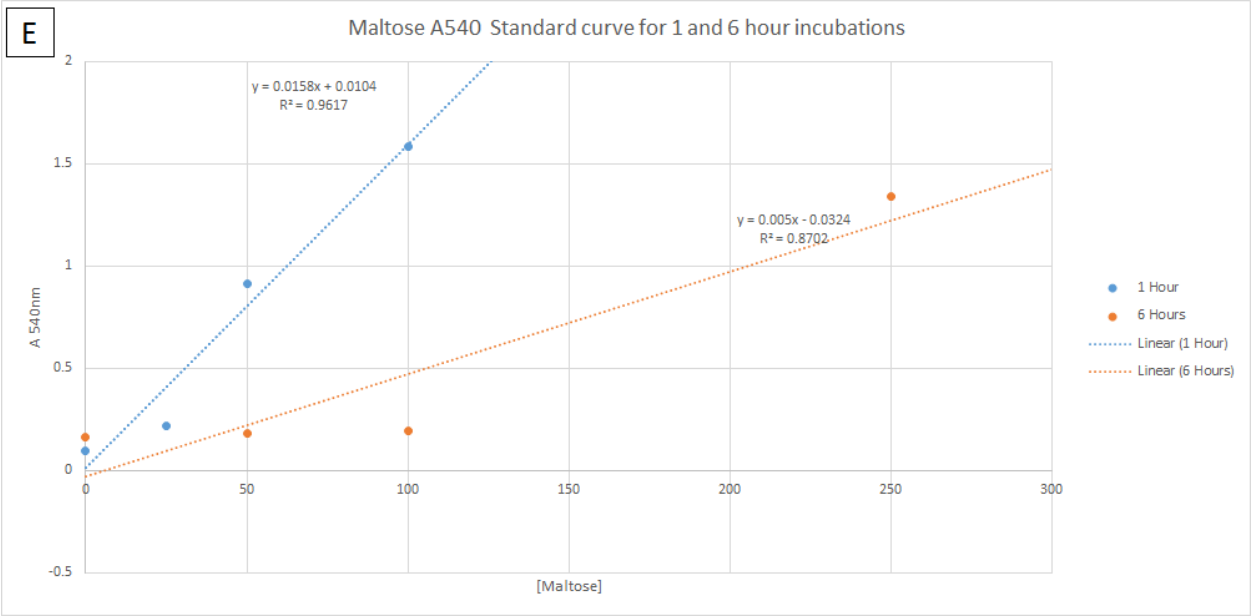

Figure 24. Absorbance at 540 nm and calculated reducing sugar release from treated faecal homogenates incubated with differing concentrations of Porcine Stomach Mucus after 1 or 6 hours. A: 540 nm absorbances after 1 hour or 6 hours (C) for autoclaved, 0.2 µm syringe filtered, and untreated mouse faecal homogenates. Buffer indicate PBS incubated with mucus as a control. B: calculated reducing sugar released to supernatant after 1 hour or 6 hours (D) of each incubation based on a maltose standard curve (E) which was run on the same 96 well plate. Each result is based on a single replicate.

Based on these results a further experiment was planned with alternative time-points (30 min and 90 min) as after 6 hours the samples had similar free sugar release and it was thought that the enzymatic progression may be more dynamic in the initial stages of the assay. This experimental set-up used triplicate replicates in order to produce more statistical analytical power. All assays were conducted using only 5% porcine stomach mucus in PBS as this was thought to be the most biologically productive from initial assays. These results are shown in Figure 25.

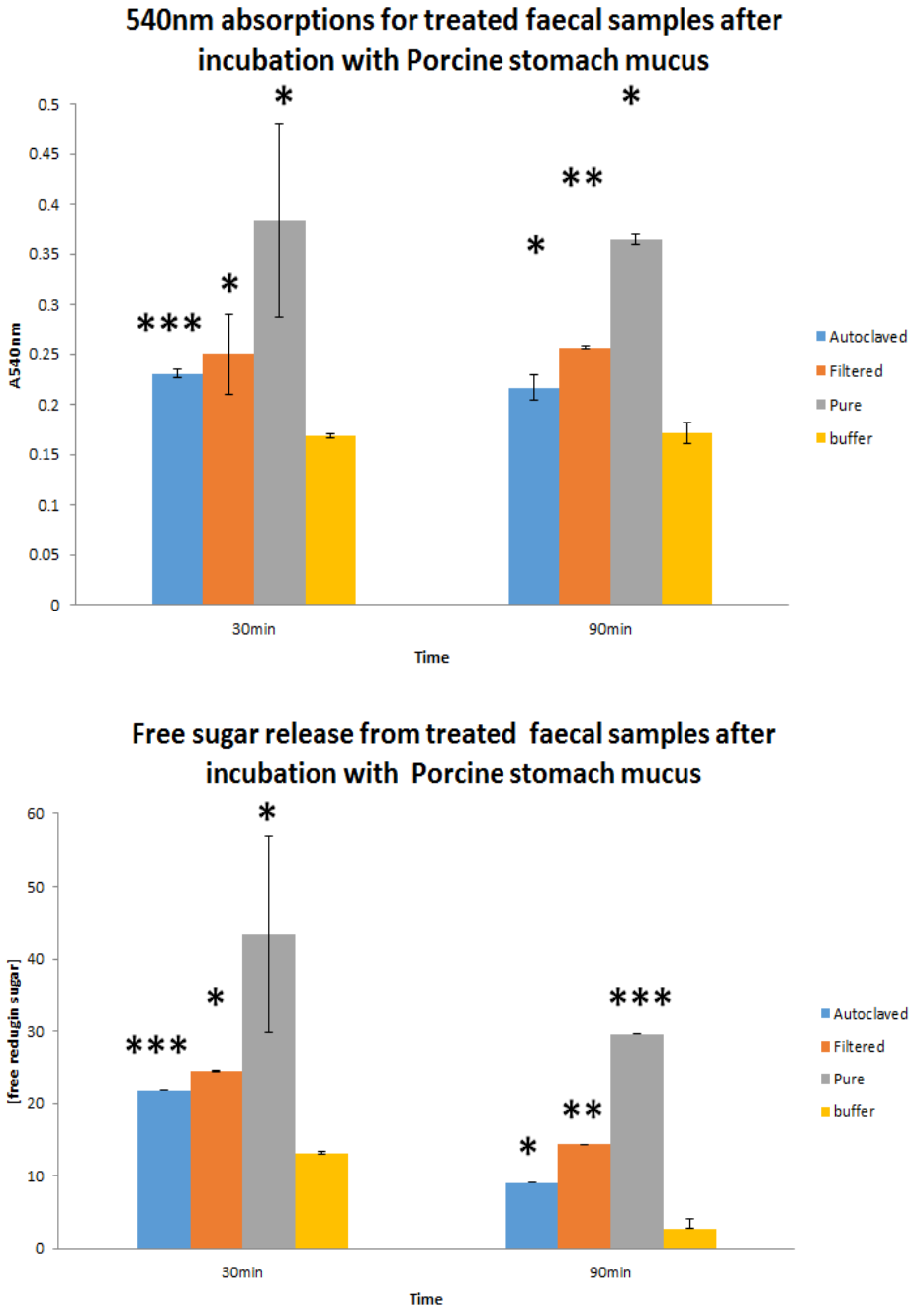

Figure 25. Upper panel: 540 nm absorbance results for 5% Porcine stomach mucus/PBS incubate with homogenised mouse faecal pellets that were either autoclaved, filtered through a 0.2 µm syringe filter or left untreated (pure). Lower panel: 540 nm absorbance converted to free reducing sugar concentrations using a standard maltose curve incubated with each sample run. Samples were incubated for 30 or 90 min before reducing sugar assay was performed using DNS and 540 absorbance measured. Using a two tailed Student's T-Test significance was evaluated for each fraction against the buffer control. P-values <0.05 are noted with a *, P-values <0.005 with ** and P-values <0.0005 with ***. Readings based on triplicate replicates.

N-acetyl neuraminic acid (NANA) release assay

A second mucinase assay was conducted based on the potential release of N-acetyl neuraminic acid (NANA) from degraded mucus as reported in Kim and Cha (2002) which is released upon degradation of side chains of peptide bonds present in the mucus complex. This assay calls for use of a 1% PSM in 0.02 M Tris-HCl solution and absorbance reading at 280 nm where free NANA is distinguishable. The results are shown in Figure 26.

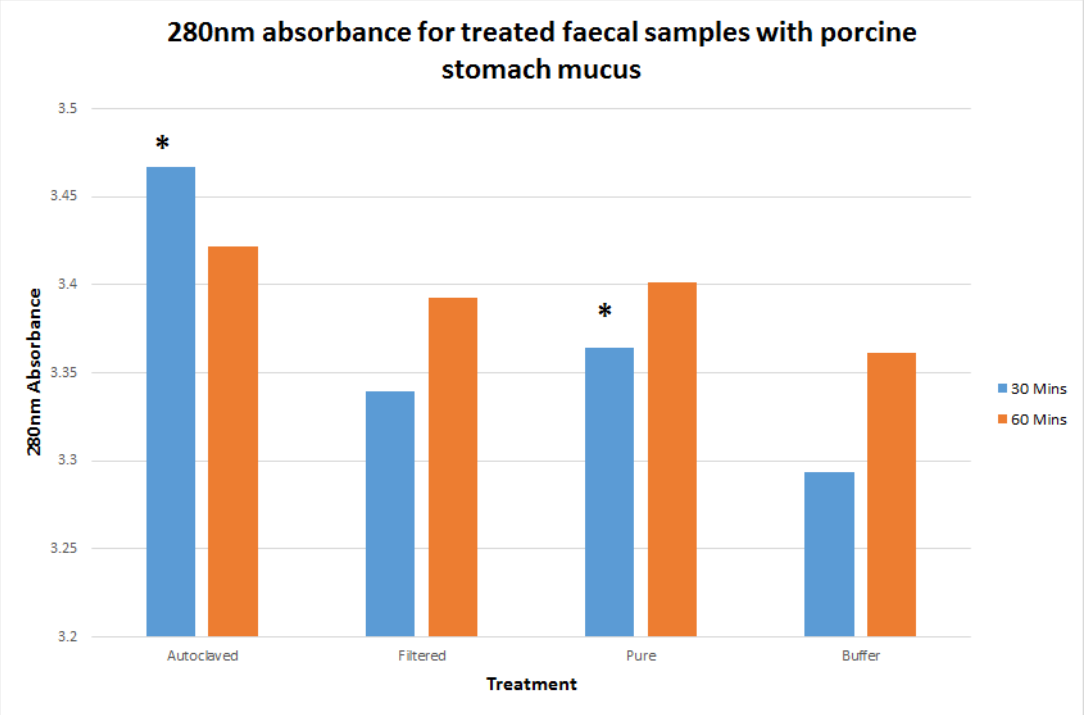

Figure 26. Absorbance values for each treatment (Autoclaved, Filtered, Pure and buffer) after 30 min (blue) and 60 min (orange) incubation with 1% PSM Tris-HCl solution. Using a two tailed Student's T-Test, significance was evaluated for each fraction against the buffer control. P-values <0.05 are noted with a *, P-values <0.005. Readings based on triplicate replicates.

Anthocyanin intervention and human faecal investigation.

Samples were evaluated both before and after PCR clean-up steps on 1.5% agarose gel apparatus, pooled and sent for sequencing (MiSeq). Ecological investigation of the returned data is beyond the scope of this study presented here.

Discussion

Immuno-histology staining and spatial organisation of Muc2 Mucin

Methacarn fixation and laser micro-dissection

Methacarn fixation of histology samples is a well-established medium for preserving structural integrity of tissues. It also allows for effective Immuno- histology staining as seen in Figure 3. However the nature of cross-linking caused by methacarn may severely inhibit penetration of bacterial cells by FISH probes and DNA stains such as DAPI, even after dewaxing steps.

DNA extraction and PCR

As seen in Figure 4, positive bands were observed in PCR products after micro-dissection of mucus in methacarn fixed histology sections. The purity of these bands, however, are questionable based on a similar strength band being observed in negative controls. To establish the accuracy of methacarn released DNA signals, samples should be prepared and sent for sequencing which will allow us to more accurately determine the ability of methacarn to deliver meaningful results from this experiment.

Naturally, samples to be sequenced should be obtained only after the decontamination steps recommended by Champlot *et al.* 2010 are conducted. We see a drastic reduction in contaminant signals in Figure 9 as a result of the more stringent preparation of PCR reagents and LMD equipment when using these recommendations. Subsequently it became standard practice in our group to use a UV cross-linker on LMD slides and reagents, as well as certain PCR reagents. Although not all contaminants were removed in Figure 9 a great majority of them were and combined with UV crosslinking allows a much cleaner protocol for LMD micro-section DNA extraction which was used extensively in subsequent experiments. In further experiments we also employed a specialised PCR cycler procedure recommended in Herbold *et al.* 2015 (see below).

dithiobis(succinimidyl propionate)(DSP) as a fixative for FISH protocols

Fluorescence in situ hybridisation comparison of PFA and DSP fixation on faecal homogenates

Both DSP and the standard fixative, PFA, produced quality images which were able to be evaluated using the DAIME programme to determine percentages of specific probe signals to the general probe and also compare intensity of signals from the two treatments. Raw images are shown in Figure 10 for PFA and DSP fixed faecal homogenates and several of such images were compared using DAIME and summarised in Figure 11.

Firstly, DSP fixation of the samples has no effect on the percentage of cells stained by the Baci731AB probe compared to PFA fixation. It is also worth noting that using the DAIME software "edge detection" feature during image analysis of either 30% or 70% appears to make little difference to the results. Significant differences are seen however in the two fixatives results in regards the percentage of EuB338 I-III pan bacterial mix-stained cells compared to the DAPI stained cells. DSP returns a slightly lower percentage of stained cells. A similar but consistent reduction in the number of cells stained with the Akk1437 probe compared to EuB338 I-III and DAPI stained cells is also seen. These differences may be due to slight differences in the microbial community from the faecal pellet, however all precautions were taken to limit these effects, i.e. mice were fed a constant diet and the pellet was homogenised as best as possible.

An additional factor that may influence the output of the DAIME software is the signal intensity recorded for each image. A lower signal intensity per cell after DSP fixation, as seen consistently in Figure 12, compared to that of PFA will give some bias to bio-volume results. If, as we see in Figure 12, DSP fixation yields lower signal intensities, when evaluating these data against a sample with higher intensities will mean a certain number of signals are dis-regarded by the software as being under threshold, where in fact they are true signals from stained populations. It is highly possible that DSP fixation has some intrinsic bias towards certain species. We have observed in our lab that DSP fixation often returns lower intensity FISH signals for Gram-positive species, possibly due to over-fixation of the cell walls. Other biochemical reasons for the loss of signal intensity should also be investigated to reveal any potential fixation bias of DSP. For the mean-time, this intensity bias of DSP goes someway to potentially explaining the discrepancies we see in the populations of EuB338 I-III pan bacterial stained cells and Akk1437 stained

cells which in turn yields lower population proportions as seen in Figure 11.

These results, although not identical for PFA and DSP fixation are highly encouraging concerning the use of DSP as a fixative. Complete and accurate FISH staining efficiencies are not guaranteed even when using PFA as a fixative, and some information is inevitably lost due to bias in hybridisation and ecological differences between species.

Immune-histology staining of Muc2 on DSP fixed colonic sections

Clearly to be seen in Figure 13 are successful immune-histology stains of the Muc2 layer in mice colons fixed using the novel fixative DSP. We can conclude from these images that DSP allows epitopes on Muc2 to remain exposed allowing for binding by specific anti-Muc2 antibodies as performed in this present study. The thickness of the sections (16 µm) made a composite "Z- stack" of the section necessary to image the entire Muc2 layer whereby Muc2 production in goblet cells could be seen as well as its secretion into the lumen. The epithelial layer retained its structural integrity, however we suggest that luminal contents and the mucus layer have much lower structural formation and for that reason sank and compressed into the slide, making Z-plane imaging a requirement.

Immune-histology staining of clinical samples is of vital importance in microscale organisation studies. Allowing to stain Muc2 in this way allows us to more specifically target bacteria within, outside or at the interface of the mucus layer. What is not known at this point is how DSP may affect other more specific epitope targets, for example if they themselves contain primary amine groups which would be bound to by DSP. An area of further study would therefore be necessary to evaluate DSP's usefulness for immune-histology staining of a variety of other potential immune targets.

Mapping Akkermansia across a fixed colon section

As the conjugated images show in Figures 14 and 6, two colon sections were investigated from the same colon and less than 50 µm downstream of each other. This makes for an extremely powerful set-up to investigate different methodologies and the results they produce in terms of microbial composition.

From the section destined for FISH analysis using CLSM, more than 200 images (see Figure 14 for one example) were deemed suitable for further analysis using the DAIME software. Images were discarded

before analysis based on whether more than 5% had visible DAPI signals or more than ~95% epithelial coverage. Analysis of these images in DAIME consistently showed an average relative abundancy of *Akkermansia* in regards to EuB338 I-III pan-bacterial stained cells of between 10 and 20%. This is consistent with other reported findings both here and elsewhere. However we must remember the major limitation of these Figures is that they are based on relative abundance within the EuB338 I-III pan bacterial stained population. Although cells stained with DAPI would be likely to be stained by EuB338 I-III we cannot assume that EuB338 I-III has covered the entire microbial biomass and may therefore have skewed these findings. Also, as predicted, there is a huge variety of *Akkermansia* distribution even within one cross section of one colon, ranging from 0.1% to 50.7%. However the mean values for both "lumen" and "epithelial proximal" sections were very close at 12.5%.

We then sought to compare the relative abundances of *Akkermansia* from a PFA fixed colon to the relative abundances of reads from sequenced micro- dissects from the same colon. Figure 16 summarises the two experiment's results. Firstly, we can see a huge variety of the abundance of *Akkermansia* in these 4 samples, ranging from 23.2% (sample 11) to >0.01% (sample 23). This variety is, however, not due to lower total bacterial populations as shown in Figure 17 whereby total populations also vary greatly.

To summarise then, FISH analysis of one colon section, fixed with standard fixative-PFA, yielded a total *Akkermansia* population of 12.5%. Sequencing data from a section of the same colon, fixed with the novel fixative DSP, yielded a total *Akkermansia* population of 15.7% from sequence data. When assessing sequence data for *Akkermansia* and in-fact any bacteria it is important to remember that many species harbour differing copy numbers of the 16S rRNA gene which will inevitably skew results in favour of species with higher copy numbers. *Akkermansia muciniphila* has itself 3 copies of this gene (**rrndb.umms.med.umich.edu**) which will affect the accuracy of the sequencing results, compared to other species.

By fixing both sections with DSP we were able to reduce bias in regards of signal intensities that were shown in "*Fluorescence in situ hybridisation comparison of PFA and DSP fixation on faecal homogenates",* specifically, Figure 12.

These results are encouraging in terms of the use of DSP as a reversible fixative giving reliable sequence information which truly reflects microbial composition. Naturally a larger number of DSP fixed micro-dissects should be investigated to overcome any micro-geographic bias present in this sample. A further line of inquiry to be followed to bolster the DSP case would be to compare sequence results from

a faecal pellet homogenised and fixed DSP and PFA as well as a non-fixed sample and send micro-dissections of these for sequencing. This would allow us to determine the accuracy of DSP sequence results compared to a non-fixed sample, as some species may be less susceptible to fixation and/or DNA extraction than others.

Semi-quantitative distribution of Akkermansia in colons of mice on two diets

Based on previous studies and observations, we hypothesised that powdered normal chow fed mice would exhibit a higher proportion of *Akkermansia* in their colons compared to mice fed on the same diet in pellet form.

Importantly, in Figure 18 the total bacterial load shows no significance differences between the powder and pellet diets which indicates that differences in *Akkermansia* populations are not dependent on total sample populations. We can also see in Figure 19 that powder diet fed mice have higher *Akkermansia* populations (average 4.13% relative abundance) compared to the pellet fed mice which have no detected *Akkermansia* reads at all.

The results shown in Figure 19, however, do not entirely agree with those in Figure 16. The micro-dissect sample *Akkermansia* populations shown in Figure 16 have an average *Akkermansia* relative abundancy of 15.7%, whereas, Figure 19 yields an average of 4.13% relative *Akkermansia* abundancy. The reasons for the discrepancy between these two sections is not clear. Both sections used are from the same colon and less than 100 µm downstream of each other, we would have expected the populations to be fairly comparable. The cause of this discrepancy is unclear however it is not likely to be due to DSP fixation bias as both sections were fixed and treated with the same DSP protocol. We could also assume that, although sections were as proximal to each other as possible, that micro-geographical factors are influencing community composition, even on sections less than 100 µm apart. This is entirely plausible given our own previous results shown here show differing compositions of microbes at the mucinal interface compared to areas just a few µm into the lumen.

Although different community structures are visible in Figure 7, the quality of FISH images able to be captured by our LMD setup does not allow for reliable DAIME quantification. If this were possible we would be able to analyse relative abundancies in the FISH images and compare them directly to the sequence data retrieved subsequently. Many FISH probe fluorophores return sub-optimal results when visualised with

air objectives due to rapid bleaching. Oil or glycerol immersion objectives are also not possible to use in a LMD setup as the micro- dissecting laser would be rendered useless. A third possible solution to this problem, which we attempted to utilise, would be to create an LMD "sandwich" in which two slides are layered back to back with the section immersed in a liquid medium, which would allow certain fluorophores to remain viable during acquisition. This proved to be a technically difficult method which was unable to remedy many problems. Of particular concern was in laser micro-dissection in which capture of sections was extremely difficult. We also had concerns with contamination across the section due to the liquid layer covering it.

Figure 20 was produced in an attempt to explain and better visualise microbial community structure variations based on diets. Panel A of Figure 20 implies that much of the variation between study arm clusterings may well be driven by contaminations found in the controls, and possibly from FISH hybridisations, due to the fact that exhaustive samples cluster some-what away from the diet experiment samples. As a result of this in panel B the same analysis was conducted after removal of control samples. Doing so shows us again that the diet experimental samples cluster away from the exhaustive samples. Panel C is a similar analysis performed only on the diet arm of samples, and show some degree of clustering. This suggests that communities are not significantly affected by the diet. This is perhaps not surprising as both study arms are on the same diet but received it in a different form. It seems based on data presented here that *Akkermansia* is drastically affected by this subtle difference but the proportions and presence of other species is affected less so. An important line of future research would therefore be in investigating which other species are as affected as dramatically and eventually any clinical significance. A similar pattern is observed when all samples are evaluated against each other, with few correlations between samples.

Species showed to be enriched in the diet experimental arms were form the candidate division TM7 and the hgcl clade of the *Sporichthyaceae*. TM7 division bacteria have been found in a variety of environments, including human saliva and skin, and may be associated with mucosal inflammation (**He *et al.* 2014**). The S*porichthyaceae* are thus far only described in fresh water systems (**Newton and McLellan 2015**). These two groups are in greater numbers on average in the diet intervention samples (47% and 66% increase respectively) compared to exhaustive samples. It is likely to be due to contamination of the diet samples during FISH hybridisation. However it is important to investigate both the source and nature of these potential contaminants, so as to be sure that they are indeed that, and not important members of a shifter microbial community in the colon.

The reasons for higher *Akkermansia* populations in colons of mice fed on powdered diets are highly complex. The most likely explanation is that a powdered diet has much greater access to compounds to both the host digestive system and microbial players in the intestines. Higher accessibility to compounds in the diet and therefore higher and faster uptake would mean faecal matter entering the colon will have fewer readily utilisable compounds able to be utilised. In effect this could create a "starved" colon environment whereby *Akkermansia* would be able to out-compete other microbes as they are feeding on a continuously available substrate, i.e. mucus and thereby infiltrate further into the lumen to harvest other complex molecules that would not normally be available to it.

It is also worth noting that samples were taken in both cases from the lumen only, which helps to explain the total lack of *Akkermansia* reads from the pellet diet colons. Had we dissected samples from closer to the mucus layer a higher abundancy of *Akkermansia* reads may have been reported, partly for the reasons given above concerning a "starved colon". In the pellet diet colons we may expect a greater number of microbes metabolising complex and simple molecules in the lumen, which may out-compete *Akkermansia* and it may therefore remain in its more specialised niche of mucus degradation. The above experiments could be performed again taking a greater number of samples from both sections as well as comparing mucus layer samples to evaluate this hypothesis.

FISH probe design against the* Erysipelotrichaceae *family

In silico FISH probe design

The resulting probe ALBA365 targeting a large part of the *Allobaculum* genus, a member genus of the *Erysipelotrichaceae* family, was tested *in silico* for a number of traits. Using the ARB-SILVA databases the probe was shown to have 770 perfect matches of which 84 were non-*Allobaculum* hits. This represents about 90% of the known *Allobaculum* genus. Of potential single-base pair mismatches to the probe, the vast majority had a mismatches cytosine base at position 1 of the target sequence. Based on this the competitor probe cALBA365 was also designed wherein a guanine is supplemented in the corresponding probe position to preferentially bind to these non-target groups, thus blocking any potential signal from mismatched ALBA365.

In vitro probe evaluation

After hybridizing colon sections, at different formamide concentrations, from a single mouse with ALBA365 Cy3 and cALBA365-unlabeled and with EuB338 I,II,&III CLSM images were produced and analysed using the Formamide curve function in DAIME. Percentage coverage of the probes were also evaluated the results are shown in Figures 22 and 23. Figure 21 also shows some examples of hybridisations with and without EuB 338 I, II,&III Fluos, and from this we can conclude that the cells stained are indeed identical in morphology to known *Allobaculum* species and are consistently so throughout the entire formamide curve.

Initially we hybridized cecal homogenates with ALBA365 and cALBA365 over a range of formamide concentrations (Figure 22). The intensity of each signal was analysed over this concentration curve and assessed in DAIME and shows an optimal formamide% in the hybridization buffer between 0% and 10%. In the same Figure we also calculated the percentage of cells stained by ALBA365 as a function of cells stained by DAPI giving an average population at 3.7%, which is stable over all formamide concentrations which allows us to assume that only signal intensity is affected by formamide. The signal intensity is essentially a measure of the binding strength and number of probes to the 16S rRNA subunit and formamide increases the melting probability of the probe from the subunit. By producing a curve of formamide concentrations we can assess at what concentration the probe no longer binds to the subunit efficiently. As the total population of stained cells remains stable through different concentrations we see that only the number of probes per cells is altered and not the specificity of the probe to the target organism group.

We repeated the formamide curve under the same conditions with the addition of an EuB338 I-III pan bacterial probe. The proximity of the EuB338 I-III and ALBA 365 target sequence on the 16S rRNA subunit may have resulted in altered binding efficiency of ALBA 365. Binding to the 16S rRNA by one probe may result in conformational changes in the secondary structure of the subunit which could either occlude binding sites of other probes or open up sites for those probes. Results shown in Figure 23 allow us to conclude that EuB338 I-III does not affect ALBA365 binding. The formamide curve shown in Figure 23 is similar to that shown in Figure 22 with no EuB338 I-III probe, with an optimal formamide concentration between 0 and 10%. The population percentages stained by ALBA365 are also comparable to those in Figure 22 with an average ALBA365 population in DAPI of 4.5% and an average of ALBA365 stained populations as a percentage of EuB338 I-III stained cells of 4.7%. Additionally the percentage of EuB338 I-III stained cells as a function of DAPI stained cells is high, 95.4%, showing also that ALBA365 does not affect EuB338 I-III probe hybridization due to secondary structure alterations of the subunit.

The average stained cell numbers by ALBA365 is considerably lower than what would be expected from sequencing results where a population closer to 25% was observed (not shown). The reasons for this may be due to probe specificity for large groups within this 25% that are not targeted by the probe, and thus only staining a smaller number of cells in the sample. A deeper assessment of the populations present in the *Allobaculum* designated samples in the sequencing results would allow to assess if the majority of these samples fall outside the *Allobaculum* species covered by the probe ALBA365. Alternatively the copy number of 16S rRNA gene operons in the genus could shift 16S rRNA sequencing results. No *Allobaculum* genus member has yet had its entire genome sequenced, however other members of the *Clostridia* have copy numbers between 1 and 7 and *Allobaculum* may well harbour multiple copies which will over-estimate their numbers in any sequence data approach.

These results presented here make in-roads into our ability to have confidence in using ALBA365 for FISH based experiments. To further increase confidence a further formamide curve should be produced with a higher resolution using smaller formamide concentration intervals, i.e. 0%, 5%, 10%15%. This will allow us to further optimize the formamide hybridization buffer to give optimal staining of samples.

Mucinase assay development

Free sugar release assay

The free sugar release assay is dependent on faecal homogenates being able to break down porcine stomach mucus (PSM) and release reducing sugars from the complex molecules therein. Figures 24 and 25 summarise two approaches made in evaluating the ability of faecal homogenates to release reducing sugars when incubated with mucus. Figure 24 represents our attempt at an exploratory assay to better understand the basic dynamics of mucus break- down to further direct our investigative efforts.

Zero % mucus addition in all panels in Figure 24 allows us to determine that the concentration of free-reducing sugars in the buffer, autoclaved, filtered and untreated samples were all equally low at around 5 µg/100 µl. Incremental increase in the concentration of PSM showed a similar increase in free sugars in all treatment arms with the autoclaved and untreated samples showing a small, but statistically non-significant increase compared to the corresponding buffer controls in both 1 and 6 hour incubations. The 6 hour incubations show a progressively higher concentration of sugar release, up to a maximum of

~ 320 µg/100 µl. As both buffer controls and treatment arms show progressive increases in free sugar release over time and concentrations we can assume that some mechanism of sugar release is operating whereby the mucus is degraded independently of microbial activity. It was therefore decided to refine the time- points measured to a shorter window, as the one hour incubations showed higher variety in sugar release compared to 6 hours.

Figure 25 summarises the free sugar release after incubations with 5% PSM solution for 30 and 90 min. Of the three experimental arms the autoclaved samples showed increased free sugar release compared to the buffer control, yet lower concentrations to both the filtered and untreated samples. The reason for free sugar release from the autoclaved sample is likely due to microbial death as a result of autoclaving causing stored sugar molecules to be released or degraded from other molecules in the faecal sample during this process. The filtered sample also shows similar patterns with a slightly increased sugar release compared to the autoclaved sample. The filtered sample is theoretically also devoid of microbial players in the faeces, however secreted enzymes and effector molecules from these microbes will be able to pass through the 0.2 µm filtering step and may be able to degrade the PSM. It is also clear that PSM solutions contain free sugars, or mucins degrade over time, shown by increasing concentrations detected in the buffer solutions which increase over time and with higher percentage PSM incubations. Many microbial communities and individuals may release mucin degrading molecules into their environment in order to utilise cleaved mucus molecules as an energy source. As mentioned previously (see **Johanssen *et al.* 2008**) mucin degradation is also likely to be performed by secreted host effectors which proteolytically cleave mucins, these effectors may also still be present in the faeces and continue to function when incubated with PSM.

Such host derived effectors could also therefore be present in the untreated “pure” faecal homogenate, however the increase in free-sugars cannot be attributed to them alone. Clearly the untreated samples had a higher release of free sugars from the PSM incubations and the evidence strongly points to a role of active microbial players as well as endogenous enzymes found in the faeces. After 90 mins a highly significant increase is shown (p value < 0.0005) compared to the buffer control, a similar pattern, with lower significance is seen after 30 min. The higher standard deviation seen after 30 min of this incubation points to a highly active faecal microbial community breakdown mucus and/ or utilising free sugar released in a highly dynamic manner. This may be supported by the lower free sugar concentrations seen after 90 min as microbes may be utilising the released sugars for their own metabolism and thus lowering the concentration in the wells, which may also account for low values in

the 6 hour incubations.

This assay shows us that mouse faecal communities are able to release reducing sugars when incubated with PSM within 30 min, it does not allow us to identify a mechanism of mucin degradation, if indeed mucus is the source of these reducing sugars. Polysaccharides and other molecules found in faeces may also be the source of these sugars as bacteria metabolise them. This image may be reinforced when we remember that faecal homogenates are incubated with a mucus source taken from the stomach, and we are therefore incubating microbes and potential metabolites from completely different ends of the GI tract. Even if faecal microbes are metabolising PSM we would be unlikely to find the same players functioning in the stomach due to the much lower pH there, and may therefore have little clinical significance. To counter this effect it would be prudent to incubate luminal contents from a specific area in the colon with mucus derived from the same area. Furthermore the assay presented here does not allow us to characterise which, if any, microbes are active in mucin degradation. To improve the assay pre- and post-incubation samples could be sequenced to evaluate which species or groups proliferate during incubation with mucins. After this a simple FISH protocol could be developed using probes specific for species with potentially increased reads to confirm their presence and quantify their proliferation while also elucidating any micro-structures and micro-geographies of species.

However, as mentioned, this assay was used to evaluate the possibility of detecting mucin degradation from incubations with easily harvested, and repeated, faecal pellets, and in this we have results which allow us to continue with development of this idea. Based on this general assay we set about narrowing down the mechanism of mucin degradation by assessing more specific breakdown products in a similar manner.

N-acetyl neuraminic acid (NANA) release assay

As an alternative proxy for the breakdown of mucin, NANA is a good candidate for easy bench-based mucinase assay activity in environmental samples. Figure 26 summarises the results of this investigation as to the suitability of the NANA assay used in Kim and Cha (2002) for use in determining murine faecal mucinase ability.

From the summarised observations in Figure 26 we can first determine that after 30 min only the autoclaved and untreated samples showed an increase in absorbance at 280 nm compared to the buffer, and all samples absorbed at 280 nm similarly after 1 hour. After one hour we would suggest that any processes taking place have equilibrated, and hence we shall focus on the 30 min time-point.

The confusing increase in absorbance at 280 nm in the autoclaved samples is possibly to be due to breakdown, modification and re-structuring of chemical compounds found in the original faecal pellet that also absorb around the 280 nm area. After autoclaving, a vast number of compounds could have been modified and continue to be modified after autoclaving, which have confused these results somewhat. What is clear is that bacterial mucinase activity is not a factor in explaining the increase of absorbance at 280 nm in the autoclaved fraction. The "raw" filtered sample also will have little to no bacterial mediated breakdown or metabolism of products. However a multitude of host and bacterial enzymes may still have residual activity in the assay which may release or consume compounds into the milieu and may interfere with the 280 nm absorption results. However the filtered fraction's similar absorbance to the control buffer fraction allows us to compare experimental fractions to the filtered.

Assuming the absorption readings of both the buffer and filtered fractions constitute a reliable negative control we see a small but significant increase of the 280 nm absorption values which we could assume to be due to some bacterial agent breaking down peptide side-chains of mucus and releasing NANA. This produced NANA would likely be utilised by further species as an energy source and the low absorbance could reflect a chain feeding effect whereby NANA is rapidly utilised.

Naturally it could also be that a plethora of compounds with various absorptions are produced, or already exist, in mouse faeces by a wide range of chemical and biological activates. Most notably protein will absorb at the same wavelength and therefore is likely to occlude everything else. To be able to improve this assay, a NANA standard curve should be produced to evaluate the dynamics of NANA in a porcine mucus incubation to better understand these results.

As mentioned above a key factor in this study was the absorbance range of a variety of molecules found in both the mucin suspension and the faecal homogenate. In their paper, Kim and Cha use partially purified mucinase complex derived from *Vibrio parahaemolyticus.* Here we attempted to incubate an entire microbial milieu to determine if any mucin was broken-down. This approach is likely to occlude a more subtle under-lying mechanism by overwhelming the 280 nm absorbance readings with a huge variety of other molecules. Anaerobic incubations of the samples may refine results and make them more relevant also, as the majority of bacterial species found in faeces are anaerobes.

The principles behind this method were reported in Kim and Cha (2002) and are used in that study to detect mucinase activity in vaginal commensal bacteria, in an attempt to diagnose pathogenic species in the mucosa. Also, as mentioned previously the release of NANA from mucus is facilitated via a

fairly specific chemical breakdown of peptide side-chains in the location-specific mucin structure. These factors combined mean this assay is highly specific for its intended diagnostic use and may well have no usefulness in determining the same breakdown product from a massively different biological environment as that for which it was designed.

The usefulness of this approach in determining faecal homogenate mucinase activities is not convincing at this point, much refinement of this protocol would be required to overcome the many concerns raised above before this assay will be able to be used in research. The only current use for the assay in Kim and Cha 2002 is in identifying potential mucinase complexes from isolated cultures.

Anthocyanin intervention and human faecal investigation.

After successful DNA extraction, 16S PCR amplification and subsequent clean-up steps, samples were pooled and sent for sequencing. Sequence data for this investigation were delivered to our collaborators at the faculty of food chemistry and toxicology, University of Vienna. Analysis and evaluation of these data were beyond the scope of this research presented here.

Conclusions

We have been able to show in this study the usefulness of DSP as a reversible fixative for FISH and immune-histology staining, and importantly being able to recover genetic material which yielded 16S rRNA gene sequences. Immuno-histology staining was shown to be comparable to standard fixatives. Although DSP yielded lower signal intensities during FISH hybridisation the percentages of cells stained were certainly comparable to PFA fixation. More work is needed to evaluate the reasons behind lower signal intensities for DSP to understand if this is due to certain cell wall structures are fixed in manner which biases FISH staining.

Using DSP as a reversible fixative for genetic material retrieval was also successful and allowed us to investigate the different populations of *Akkermansia* in mouse colons fed on two similar diets. DSP was able to quantitatively differentiate between samples which, through FISH images, were shown to have differing *Akkermansia* populations. More research is needed to understand the dynamics of the mouse colon based on these two (powder and pellet) diet forms, especially as *Akkermansia* has been so often linked to human health. Further investigation is also needed in regards to DSP and especially to evaluate

how accurate DSP fixed samples are in terms of sequence data.

The novel FISH probe, ALBA365 was shown here to successfully and appropriately bind to its target group, although further refinement of the FA% to be used is required, this probe has shown it usefulness in FISH incubations of the *Allobaculum* family, a potentially important family in the human gut.

This work expands our knowledge of the dynamics of the gut microbiome and its relationship with host derived products and dietary intake of the host. By evaluating the reversible fixative DSP we also open many possibilities to further expand our knowledge and accuracy in the field of human symbionts, eventually with the aim of augmenting our gut communities with potentially positive impacts on human health.

Zussamenfassung

Mit der vorliegenden Studie wollen wir das Verständnis von Darm Mikrobiome, bei Menschen und Mäusen, erweitern. Dafür haben wir die Anwendung des neuen Fixative Dithiobis (succinimidyl propionate) (DSP) erforscht. Hierfür haben wir Histologie Proben mit einem Fluorescence *in situ* hybridisation (FISH), mit dem Schwerpunkt auf den Schleim-verbündete Bakterien *Akkermansia muciniphila,* prepariert. Das Experiment wurde durchgeführt, indem wir das Biovolumen und die Intensität von FISH Signalen von Histologie Proben, fixiert mit DSP, mit Proben unter der Anwendung der Standard Fixative für solche Protocolen Paraformaldehyde (PFA)verglichen haben. Wegen DSP's reversiblen Eigenschaften als Fixativ konnten wir, durch Laser Assisted Micro-Dissection Microscopy (LMD), DNA extrahieren und die Gensequenzierung von 16S rRNA durchführen. Wir haben auch versucht eine neuartige FISH Sonde zur Anwendung gegen die *Allobaculum* Familie zu designen, da diese Familie oftmals die Werte der Diäten von Mäusen in Experimenten erhöhen. Als abschließenden Schritt hoffen wir, in Zusammenarbeit mit unseren Kollegen von der Fakultät der Lebensmittelchemie und Toxikologie an der Universität Wien, unser Verständnis über die Veränderung von bakteriellen Gemeinschaften in menschlichen Stuhlproben unter den Bedingungen einer Diät mit erhöhter Konzentration von Anthoncyanin, zu erweitern.

Wir konnten aufzeigen das DSP in bestimmten Situationen ein nützliches Fixative für FISH ist, da die Ergebnisse vergleichbar mit denen des Standard Fixativ PFA sind. DSP kann auch Proben Fixieren für Immune-Histologie Protocole. Wir konnten Genetisches Material von Mäusedärmen extrahieren, die mit DSP angereichert wurden. Dadurch konnten wir Änderungen von bakteriellen Gemeinschaften bei

Mäusedärmen, unter dem Einfluss von zwei verschiedenen Diäten, feststellen. Diese beweist die Nützlichkeit von DSP, als ein reversible FISH Fixativ. Gleichfalls wurden die 16S rRNA Gene von menschlichen Stuhlproben, von Spendern welche auf einer Diät mit erhörten Anthocyanin Konzentrationen sind, sequenziert. Diese Ergebnisse sind aber außerhalb des Rahmens dieser Studie.

Glossary of terms:

ATL- Tissue lysis buffer. **BMI-** Body mass index. **BSA-** Bovine serum Albumin. **CLSM-** Confocal laser scanning microscopy. **CTAB-** cetyltrimethyl ammonium bromide. **DAPI-** diamidino-2-phenylindole. **DEPC-** Diethylpyrocarbonate. **DMSO-** Dimethyl Sulfoxide. **DNS-** 3,5-Dinitrosalicylic acid. **dNTP-** Deoxynucleotide mix. **DSP-** dithiobis (succinimidyl propionate). **DTT-** Dithiotheritol. **FA-** Formamide. **FISH-** fluorescence *in situ* hybridization. **GI-**Gastro-intestinal. . **IBS-** Irritable Bowel Syndrome. **IgA-** Immuno globulin A. **LMD-** Laser-assisted micro dissection. **MODS-** Multiple organ dysfunction syndrome. **NANA-** N-acetyl neuraminic acid. **OCT-** Optimal cutting temperature medium. **OTU-** Operational taxonomic unit. **PBS-** Phosphate buffered saline. **PCR-** Polymerase chain reaction. **PET-** polyethylene terephthalate. **PFA-** Para formaldehyde. **PGA-** phloroglucinol. **PSM-** Porcine stomach mucus. **SCFA-** Short chain fatty acid.

Bibliography and References

Alm, E.W., Oerther,D.B., Larsen,N.,Stahl,D.A.,Raskin, L. 1996. *„The Oligonucleotide Probe database.“.* „Applied and environmental microbiology“, PP 3557-3559.

Atuma,C., Stugala,V., Allen, A., Holm, L. 2001. „*The adherant gastro-intestinal mucus gel layer: Thickness and physical state* in vivo“. **„**American Journal of Physiol. Gastroinest. Liver Physiol“. Vol. 280, PP 922-929.

Belcheva, A., Irrazabal, T., Robertson, S.J., Streutker, C., Maughan, H., Rubino, S., Moriyama, E.H., Copeland, J.K., Surendra, A., Kumar, S., Green, B., Geddes, K., Pezo, R.C., Navarre, W.W., Milosevic, M., Wilson, B.C., Girardin, S.E., Wolever, .M.S., Edelmann, W., Guttman, D.S., Philpott, D.J., Martin, A. 2014. *„Gut microbial metabolism drives transformation of Msh2-deficient colon epithelial cells*“. „Cell“. Vol. 158, PP 288-299.

Bergstrom, K.S.B., Kissoon-Singh, V., Gibson, D.L., Ma, C., Montero, M., Sham, H.P., Ryz, N., Huang, T., Velcich, A., Finlay, B.B., Chadee,K., Vallance, B.A. 2010. *„Muc2 protects against lethal infectious colitis by dissasociating pathogenic and commensal bacteria from the colonic mucosa*“. „PLOS pathogens“. Vol.6, Issue 5.

Berry, D., Stecher, B., Schintlmeister,A., Reichert, J., Brugiroux, S., Wild, B., Wanek, W., Richter, A., Rauch, I., Decker, T., Loy, A., Wagner, M. 2013. *„Host-compound foraging by intestinal microbiota revealed by single-cell stable isotope probing*“. „PNAS“. Vol. 110, PP 4720-4725.

Champlot, S., Berthelot, C., Pruvost, M., Bennett, E.A., Grange, T., Geigl, E.M. 2010. „*An efficient multistrategy DNA decontamination procedure of PCR reagents for hypersensitive PCR applications***“.** **„**PLOS one“. Vol.5, Issue 9.

Chassaing, B., Koren, O., Goodrich, J.K., Poole, A.C., Srinivasan, S., Ley, R.E., Gewirtz, A.T. 2015. *„Dietary emulsifiers impact the mouse gut microbiota promoting colitis and metabolic syndrome*“. „Nature Letters“. Vol. 519, PP 92-192.

Davies, J.R., Wickström, C., Thornton, D.J., 2012. *„Gel-forming and cel-associated Mucins: Preparation for structural and functional studies*“. In, McGuckin, M.A., Thornton, D.J. (Eds.), „Mucins: Methods and Protocols“. PP 27-47, Humana press.

Derrien, M. 2007. *„Mucin utilisation and host interactions of the novel intestinal microbe* Akkermansia muciniphila“. PhD thesis, Wageningen University.

Dethlefsen, L., Eckburg, P.B., Bik, E.M., Relman, D.A. 2006. *„Assembly of the human intestinal microbiota*“. „Trends in ecology and evolution“. Vol. 21, Issue 9.

Dwarakanath, A.D., Campbell, B.J., Tsai, H.H., Sunderland, D., Hart, C.A., Rhodes, J.M. 1995. *„Faecal mucinase activity assessed in inflammatory bowel disease using 14C Threonine labelled mucin substrate*“ . „Gut“. Vol. 35, PP 58-62.

Everard, E., Belzer, C., Geurts, L., Ouwerkerk, J.P., Druart, C., Bindels, L.B., Guiot, Y., Derrien, M., Muccioli, G.G., Delzenne, N.M., de Vos, W.M., Cani, P.D. 2013. *„Cross-talk between* Akkermansia muciniphila *and intestinal epithelium controls diet-induced obesity*“. Vol. 122, PP 9066-9071.

Fridrich, D., Glabasnia, A., Fritz, J., Esselen, M., Pahlke, G., Hofmann, T., Marko, D. 2008. *„Oak Ellagitannins supress the phosphorylation of epidermal growth factor receptor in Human colon carcinoma cells*“. „“Journal of agricultre and food chemistry“. Vol. 56, PP 3010-3015.

Galindo-Villegas, J., Garcia-Moreno, D., de Oliveira, S., Meseguer, J., Mulero, V. 2012. *„Regulation of immunity and disease resistance by commensal microbes and chromatin modifications during Zebrafish development*“. „PNAS“. Vol 109, PP 2605-2614.

Gall, J.D., Pardue, M.L. 1969. *„Formation and detcetion of RNA-DNA hybrid molecules in cytological preparations*“. „Genetics“. Vol. 63, PP 378-383.

Garcia-Garcia, E., Galindo-Villegas, J., Mulero, V., 2013. *„ Mucosal immunity in the gut: the non-verterbrate perspective*“. „Dev. Comp. Immunol.“. Vol. 40, PP PP 278-288.

He,X., McLean, J.S., Edlund, A., Yooseph, S., Hall, A.P., Liu, S.Y., Dorrestein, P.C., Esquenazi, E., Hunter, R.C., Cheng, G., Nelson, K.E., Lux, R., Shi, W. 2014. *„Cultivation of a human-associated TM7 phylotype reveals a reduced genome and epibiotic parasitic lifestyle*“. „PNAS“. Vol. 112, PP 244-249.

Herbold, C.W., Pelikan, C, Kuzyk, O., Hausmann, B., Angel, R., Berry, D., Loy, A. 2015. *„A flexible and economical barcoding approach for higly multiplexed amplicon sequencing of diverse target genes*“. „ Frontiers in microbiology“. Vol. 6, Article 731.

Janos, F., Illes, K., Corrado Balacco, G. 2011. *„Gastrointestinal inflammation may play a critical role in the pathogenesis of depression*“. „Orv. Hetil.“. Vol. 152, PP 1477-1485.

Johansson, M.E.V., Hansson, G.C. 2011. *„Keeping bacteria at a distance*“. „Science“. Vol. 334, PP 182-183.

Johansson, M.E.V., Phillipson, M., Petersson, J., Velcich, A., Holm, L., Hansson, G.C. 2008. *„The inner layer of the two Muc2 mucin dependent mucus layers in colon is devoid of baceria*“. „PNAS“. Vol. 135, PP 15064-15069.

Karlsson, C.L., Onnerfält, J., Xu, J., Molin, G., Ahrne, S., Thorngren-Jerneck, K. 2012. *„The microbiota of the gut in preschool children with normal and excessive body weight*“. „Obesity“. Vol. 11, PP 2257-2261.

Kahn, M.T., Duncan, S.H., Stams, A.J.M., van Dijl, J.M., Flint, H.J., Harmsen, H.J.M. 2012. *„The gut anaerobe Faecalibacterium prausnitzii uses an extracellular electron shuttle to grow at oxic-anoxic interphases*“. „ISME journal“. Vol. 6, PP 1578-1585.

Kim, Y.H., Cha, J. 2002. *„ Development of rapid spectrophotometric method for detecting bacterial mucinase complex*“ . „Journal of microbial biotechnology“. Vol. 12, PP 345-348.

Koeth, R.A., Wang, Z., Levison, B.S., Buffa, J.A., Org, E., Sheehy, B.T., Britt, E.B., Fu, X., Wu,Y., Li, L., Smith, J.D., DiDonato, J.A., Chen, J., Li, H., Wu, G.D., Lewis, J.D., Warrier, M., Brown, J.M., Krauss, R.M., Tang, W.H.W., Bushman, F.D., Lusis, A.J., Hazen, S.L. 2013. *„Intestinal microbiota metabolism of L-carnitine, a nutrient in red meat, promotes artherosclerosis*“. „Nature Medicine“. Vol. 19, article 5.

Kropat, C., Mueller, D., Boettler, U., Zimmerman, K., , Heiss, E.H., Dirsch, V.M., Rogoll, D., Melcher, R.,

Richling, E., Marko, D. 2013. „*Modulation of Nrf2-dependent gene transcription by bilberry anthocyanins* in vivo“. „Mol. Nutr. Food Res.“ Vol. 57, PP 545-550.

Loy, A., Arnold, R., Tischler, P., Rattei, T., Wagner, M., Horn, M. 2008. „*probeCheck- a central resource for evaluating oligonucleotide probe coverage and specificity*“. „Environemental mirobiology“. Vol. 10, PP 2894-2898.

Linden, S.K., Florin, T.H.J., McGuckin, M.A. 2008. “Mucin dynamics in intestinal bacterial infection”. “*PLOS One*”. Vol. 3, Issue 12.

Ludwig, W., Strunk, O., Westram, R., Richter, L., Meier, H., Yadhukumar, Buchner, A., Lai, T., Steppi, S., Jobb, G., Förster, W., Brettske, I., Gerber, S., Ginhart, A.W., Gross, O., Grumann, S., Hermann, S., Jost, R., König, A., Liss, T., Lüßmann, R., May, M., Nonhoff, B., Reichel, B., Strehlow, R, Stamatakis, A., Stuckmann, N., Vilbig, A., Lenke, M., Ludwig, T., Bode, A., Schleifer, K. 2004. „*ARB: a software environment for sequence data*“. „Nucleic acids research“. Vol. 32, PP 1363-1371.

Madson, E.L. 2009. “*Exclude “Unculturable” from the taxonomic microbiology literature”*. “American society for Microbiology”. Online Article.

Mantle, M., Husar, S.D. 1993. „*Adhesion of* Yersinia enterocolitica *to purified Rabbit and human intestinal mucin*“. „Infectious Immunology“. Vol. 61, PP 2340.

Metchnikoff, E. 1907. „*The prolongation of Life; Optimistic studies*“. G.P Putnam’s Sons Publishers, New York, London.

Nava, G.M., Friedrichsen, H.J., Stappenbeck, T.S. 2011. „*Spatial organisation of intestinal microbiota in the mouse ascending colon*“. „ISME“. Vol. 5, PP 627-638.

Newton, R.J., McLellan, S.L. 2015. „*A unique assemblage of cosmopolitan freshwater bacteria and higher community diversity differentiate and urbanized estuary from oligotrophic Lake Michigan*“. „Frontiers in Microbiology“. Vol. 6, Article 1028.

Oksanen, J., Blanchet, F.G., Kindt, R., Legendre, P., Minchin, P.R., O’Hara, R.B., Simpson, G.L., Solymos, P., Stevens, M.H.M., Wagner, H. 2015. „*Community ecology package*“

Ottman, N., Smidt, H., de Vos, W.M., Belzer, C., 2012. „*The function of our mirobiota: Who is out there and what do they do?*“. „Frontiers in cellular and infection microbiology“. Vol. 2, Article 104.

Ouwerkerk, J.P., de Vos, W.M., Belzer, C. 2013. „*Glycobiome: Bacteria and mucus at the epithelial interface*“. „Best practice and research clinical gastroenterology“. Vol. 27, PP 25-38.

Qin, X., Sheth, S.U., Sharpe, S.M., Dong, W., Lu, Q., Xu, D., Deitch, E.A. 2011. „*The mucus layer is critical in protecting against Ischemia/reperfusion-mediated gut injury and in the restituion of gut barrier function*“. „FIN OUT WHERE PUBLISHED“.

Quast, C., Pruesse, E., Yilmaz, P., Gerken, J., Schweer, T., Yarza, P., Peplies, J., Glöckner, F.O. 2013. “*The SILVA ribosomal RNA gene database project: improved data processing and web-based tools*”. “Nucleic acid research”. Vol. 41, PP 590-596.

Rogier, E.W., Frantz, A.L., Bruno, M.E.C., Kaetzel, C.S. 2014. „*Secretory IgA is concentrated in the outer layer of colonic mucus along with gut bacteria*“. „Pathogens“. Vol. 3, PP 390-403.

Steinbeck, J. 1939. „*The Grapes of Wrath*“. The Viking Press-James Lloyd Publishers, New York.

Stevenson, B.S., Eichorst, S.A., Wertz, J.T., Scmidt, T.M., Breznak, J.A. 2004. „*New strategies for cultivation and detection of previously uncultured microbes*“. „Applied and Environmental microbiology“. Vol. 70, PP 4748-4755.

Stoddard S.F., Smith B.J., Hein R., Roller B.R.K., Schmidt T.M. 2015. *”rrnDB: improved tools for interpreting rRNA gene abundance in bacteria and archaea and a new foundation for future development*”. “Nucleic Acids Research”. Doi-10.

Traka, M., Mithen, R. 2008. „*Glucosinolates, Isothiocyanates and human health*“. „Phytochemistry reviews“. Vol. 8, PP 269-282.

van Passel, M.W.J., Kant, R., Zoetendal, E.G., Plugge, C.M., Derrien, M., Malfatti, S.A., Chain, P.S.G., Woyke T., Palva, A., de Vos, W.M., Smidt, H. 2011. „*The genome of* Akkermansia muciniphila*, a dedicated intestinal mucin degrader, and its use in exploring intestinal metagenomes*“. „PloS one“. Vol. 6, Issue 3.

Wang, Z., Klipfell, E., Bennett, B.J., Koeth, R., Levison, B.S., DuGar, B., Feldstein, A.E., Britt, E.B., Fu, X., Chung, Y.M., Wu, Y., Schauer, P., Smith, J.D., Allayee, H., Tang, W.H.W., DiDonato, J.A., Lusis, A.J., Hazen, S.L. 2011. „*Gut flora metabolism of phosphatidylcholine promotes cardiovascular disease*“. „Nature“. Vol 42, PP 57-65.

Xiang, C.C., Mezey, E., Chen, M., Key, S., Ma, L., Brownstein, M.J. 2004. „*Using DSP, a reversible cross-linker, to fix sections for immunostaining, microdissection and expression profiling*“. „Nucleic acids research“. Vol. 32, Article 22.

Yilmaz, L.S., Haroon, M.F., Rabkin, B.A., Tyson, G.W., Hugenholtz, P., 2010. „*Fixation-free fluorescene* in situ *hybridization for targeted enrichment of microbial populations*“. „ISME journal“. Vol. 4, PP 1352-1356.

Yilmaz, L.S., Parkernar, S., Noguera, D. R. 2011 “*mathFISH, a Web Tool That Uses Thermodynamics-Based Mathematical Models for In Silico Evaluation of Oligonucleotide Probes for Fluorescence In Situ Hybridization*”. “Applied and Environmental Microbiology”. Vol.77, PP 1118-1122.

Zhu, Y., Jameson, E., Crosatti, M., Schäfer, H., Rajakumar, K., Bugg, T.D.H., Chen, Y. 2014. „*Carnitine metabolism to trimethylamine by an unusual Rieske-type oxygenase from human microbiota*“. „PNAS“. Vol. 111, PP 4268-4273.

Acknowledgments

The most important person to thank for this entire project is, of course Orest, who sadly won't ever see the finished project of his help and support during the writing of this thesis. This thesis is as much Orest's as it is mine. I'd then like to thank David Berry and Alex Loy, who kindly let me conduct my thesis in thier lab, but also for thier support be it scientific, administrative or personal. The entire DoME community is possibly the only reason I was able to survive this masters and many of them have become good friends. Particular thanks goes to those who were able to, or tried to, help me when I had no idea what I was doing, including Michi Steinberger, Bela Hausmann, Markus Schmidt, Buck Hanson, Petra Pjevac, Ken Wasmund and anyone else who found me confused in the lab, which is practically the whole DoME family.

I want to take the oppertunity to also thank the department for the way the death of my good freind Orest was dealt with. Michael Wagner, Dagmar Woelbken and Matthias Horn handeled the situation extremely well and in retrospect helped us all through a difficult period. During this period Lena König, Julia Vierheilig and Hannes Schmidt were there for me, and made a huge difference to me at the time, and for that I thank them deeply.

Lastly, but by no means leastly, I want to thank my friends, family and colleagues at Labors.at who had the patience to listen to my whining when I needed to vent, including, but not limited to Monika Braunsteiner, Andrea Leukauf, Emma Baarde, Zjelka Matosevic and Margit Apostol.

Curriculum Vitae

Name: **Owen Williams**
Qualification: **BSc**
Nationality: **British**
Languages: **English (Native)**
German (Fluent)

Education and Qualifications

- **Oct. 2013 – Present.** Masters in Molecular Microbiology, Immunobiology and Microbial Ecology
  University of Vienna
- **Oct. 2007 – Jul. 2011** Bachelors in Biology (with a year in Europe).
  Imperial College London and Universitá degli Studi di Padova (Italy)
- **Sept. 2004 – Jul. 2007** 3 A-Levels- Human Biology (B), Chemistry (A), History (A) and 1 As-Level in Psychology
  Yale 6th Form College, Wrexham
- **Sept. 1999- Jul. 2004** 11 GCSEs grade A-C in, Double award Science, English Literature and Language, Mathematics, French, Welsh, ICT, Music, History and Religion
  Rhosnesni High School, Wrexham

Work experience

Jan. 2012-Apr. 2015 Gruppenpraxis labors.at Pathology laboratory, Vienna, Austria
Biomedical analyst

Sept. 2008-Jul 2011 University of London Royal Navy Unit (LURNU)
Senior Midshipman

Sept. 2004-Apr. 2010 Techniquest@Glyndŵr science museum
Presenter/Explainer